Resuscitation of Bacterial Biofilm by Sunlight: Effects on Different Enteropathogenic Bacteria

By:

Mrinal Chandra Chanda - 19236002

Partha Pratim Arjya - 19236016

Nusrat Kabir Trisha - 19236009

Mohammad Daniel - 19236013

A thesis submitted to the Department of Mathematics and Natural Sciences in partial fulfillment of the requirements for the degree of Bachelor of Science in Biotechnology.

Department of Mathematics and Natural Sciences

BRAC University, Bangladesh

May 2024

Declaration

It is hereby declared that

1. The thesis submitted is our own original work while completing Bachelor of Science degree at BRAC University.

2. The thesis does not contain material previously published or written by a third party, except where this is appropriately cited through full and accurate referencing.

3. The thesis does not contain material which has been accepted, or submitted, for any other degree or diploma at a university or other institution.

4. We have acknowledged all main sources of help.

Student's Full Name & Signature:

Student Full Name Student ID	**Student Full Name** Student ID
Student Full Name Student ID	**Student Full Name** Student ID

Approval

The thesis titled "Resuscitation of Bacterial Biofilm by Sunlight: Effects on Vibrio cholerae, Shiga Toxin Producing Escherichia coli" submitted by

Mrinal Chandra Chanda

Partha Pratim Arjya

Nusrat Kabir Trisha

Mohammad Daniel

has been accepted as satisfactory in partial fulfillment of the requirement for the degree of Bachelor in Biotechnology on

Examining Committee:

Supervisor:

(Member) _____

Iftekhar Bin Naser, PhD

Associate Professor,

Department of Mathematics and Natural Sciences,

BRAC University

Program

Coordinator: _____

(Member) Iftekhar Bin Naser, PhD

Associate Professor,

Department of Mathematics and Natural Sciences BRAC University

Departmental

Head: (Chair)

_____

Chairman and Professor,

Department of Mathematics and Natural Sciences,

BRAC University.

Ethics Statement

This material is an original work, which has not been previously published elsewhere. It is my own research and analysis in a truthful and complete manner. The paper properly credits all the sources used (correct citation)**.**

Abstract

There is significant evidence that suggests that bacteria go through various mobile and immobile phases during their lifetime. All these various phases, in turn, facilitate the pathogenic bacteria to cause and spread diseases during the seasonal outbreaks. These reversible mobile and immobile phases in bacteria are most evidently seen through the making and then the breaking out of biofilms. Many environmental factors induce bacteria to enter a sessile state in the form of biofilms, while many cause them to break out those biofilms and become activated i.e, pathogenic. In this study, we focused on the effect of sunlight as a factor for the bacteria to break out of those biofilms and be resuscitated to cause diseases. Biofilms of a number of *cholera* strains and shiga toxin producing *E.coli* that cause diseases during the months of March to July were subjected to sunlight throughout the winter season (December to February) using four different phases, i.e., methods of data collection and its effects were observed and analyzed using appropriate statistical analysis. The resulting data and statistical analysis suggests that biofilms in the winter sunlight do not get resuscitated and a significant amount of planktonic bacteria does not come out of the biofilms to cause diseases. As a result, during the winter seasons, the incidence rate of some of the diseases may stay low as the causative bacteria in the waters stays immobile within the biofilm structures. However, in order to provide any conclusive evidence, round the year study including more samples is required.

Acknowledgement

First of all, we wish to declare our humble gratitude to Almighty, who has bestowed the gift of utmost mercy, and given us the strength, patience and understanding required to complete this work.

We convey our special thanks to Professor A. F. M. Yusuf Haider, PhD, Chairman, Department of Mathematics and Natural Sciences, BRAC University, who always has tremendous support for every student. We express our gratitude to our supervisor, Dr.Iftekhar Bin Naser, PhD, Associate Professor, Department of Mathematics and Natural Sciences, BRAC University, for his encouragement and continuous guidelines for this research. Additionally, we are grateful to Afia Nawshen, Former Lecturer, Department of Mathematics and Natural Sciences, BRAC University, for always guiding us and mentoring us throughout the project. We are indebted to all the extraordinary people of the Life Science Laboratories, BRAC University. Without their all-time support this would not be completed. We would like to specially recognize Asma Afzal, Lab Officer, and Tanzila, Nadira and Ashiq, Lab Assistants, Life Science Laboratories, BRAC University for being so patient and helpful towards us for the entirety of the project. We would also like to express our deepest respect to Mahboob Hossain, PhD, Professor, Department of Mathematics and Natural Sciences, BRAC University for always being a great inspiration.

We sincerely thank our beautiful family who trusted in us and are always there for us. This journey would be incomplete without the support of all of our well wishers. We are very grateful and indebted to all of these people.

Sincerely,

Mrinal Chandra Chanda

Partha Pratim Arjya

Nusrat Kabir Trisha

Mohammad Daniel

Department of Mathematics and Natural Sciences, BRAC University.

Table of Contents

List of Figures

List of Table

List of Acronyms

EPS- Exo-Polysaccharide

VPS- *Vibrio* Polysaccharide

CVEC- Conditionally Viable Environmental Cell

VBNC- Viable But Not Culturable

OD- Optical Density

ELISA- Enzyme-Linked Immunosorbent Assay

EIA- Enzyme Immunoassay

RIA- Radial Immunoassay

ELISPOT- Enzyme Linked Immuno Spot Assay

HUS- Hemolytic Urine Syndrome

HC- Hemorrhagic Colitis

CTX- Cholera Toxin

ER- Endoplasmic Reticulum

AFR6- ADP ribosylation factor6

Monophosphate PKA- Phospho Kinase

CFTR- Cystic Fibrosis Transmembrane Receptor

LPS- Lipopolysaccharide

STX- Shiga Toxin

PP- Peyer's Patch

LB- Luria Broth

LA- Luria BertaniAgar

QS- Quorum sensing

CAI-1- Cholerae autoinducer-1

AI-2- Autoinducer-2

VPS- Vibrio Polysaccharide

HCD- High Cell Density

LCD- Low Cell Density

LSR- Lipolysis Stimulated Lipoprotein Receptor

HapR- Hemagglutinin Protease Regulatory Protein

aW- Water Activity

TCBS- Thiosulfate-citrate-bile salts-sucrose

TSI- Triple Sugar Iron

CBB G-250- Coomassie Brilliant Blue G-250

CFU- Colony Factor Unit

STEC - Shiga Toxin-Producing *E. coli*

Chapter 1: Introduction

1.1 Background:

Cholera and diarrhea outbreaks in Bangladesh are more common in the summer and less common in the winter because of the country's tropical climate. In order to validate the cyclical increase and reduction in infections induced by the underlying causes of these disorders, several factors have been explored. The role of bacterial biofilms in this phenomenon has received considerable attention.

Toxigenic Biofilm-associated *Vibrio cholerae* persists in cholera-endemic locations, with the bacteria firmly embedded in an exopolysaccharide matrix. It's not uncommon for cells in a biofilm to enter a quiescent state, giving rise to conditionally viable environmental cells (CVEC) that are difficult to develop in a laboratory. However, these cells can reactivate into the planktonic form naturally through a variety of means, proliferate, and cause cholera epidemics (Naser et al., 2017). Many of these methods have been investigated as potential candidates that resurrect the cholera bacterial biofilms and release the planktonic bacteria, thereby causing infections and, on a larger scale, epidemics. However, research on the role of sunshine in reviving bacterial biofilms and triggering seasonal epidemics of cholera in Bangladesh is still lacking.

Because sunlight is not as strong or as persistent in the winter, it is reasonable to assume that bacterial biofilms are not broken to release the planktonic bacteria that cause cholera infections during this time of year. Bacteria like *Vibrio cholerae* and *Shigella enterocolitica* (STEC) can overwinter within biofilm formations, where they will not multiply and spread disease.

1.2 Aim of the study:

The purpose of this research is to find out if bacterial biofilms may be resuscitated by winter sunlight and planktonic bacteria can escape. Seasonal epidemics are common for many diseases, including cholera. Possible explanation for the relative lack of winter outbreaks: less sunshine in the winter means less degradation of biofilm.

Chapter 2: Literature Review

2.1.1 Biofilms:

Biofilms are a type of microbial surface composed of a matrix of complex polymeric substances (EPS) that many different types of bacteria stick to for protection. This is done in reaction to stress or other adverse environmental consequences so that the bacteria can live even in these settings. An auto-inducer, a quorum sensing signal molecule, triggers the secretion of EPS, which in turn leads to the development of a unique three-dimensional biofilm architecture, all within the context of a developmental process known as biofilm formation. Bacteria may use biofilm formation as a means of protection against environmental threats such antibiotics, heat stress, and predators. The infectious dosage of a disease may be contained in a biofilm consisting of as few as 1.0x109 cells per clump (Huq et al., 2008). Biofilm generation by pathogenic *Vibrio cholerae* has been shown to help the pathogen's persistence in the environment, particularly in aquatic settings where adhesion to surfaces plays a key role in the pathogen's ability to spread and cause epidemics. Biofilms can contain highly variable local microenvironments, where organisms compete for resources in the face of challenges such limited food supply, fluid mobility, desiccation, poisonous chemical gradients, ultraviolet (UV) radiation, and changes in pH and temperature. Therefore, biofilm development is a straightforward microbial survival strategy where microorganisms, including pathogens, reside in a dynamic equilibrium where cell clusters grow, mature, and detach to disseminate to other surfaces (Hall-Stoodley & Stoodley, 2005). One or more bacterial species can form the three-dimensional structure of a biofilm. They can be found anywhere, from lake water and raw food to sewage pipes and kitchen sinks to animal teeth and laboratory equipment. Biofilms are frequently called "slime" by the general public. Within this slime, however, a novel and sophisticated system emerges, one that is both stable and plays a crucial role in the survival and pathogenicity of bacteria.

2.1.2 Biofilm Development:

Proteins, polysaccharides, lipids, and DNA come together to form a matrix that shields bacteria and allows them to thrive in the environment. The volume of a biofilm might be anywhere from 10-30% microorganisms. About 97% of the biofilm is water, and it is water that carries the nutrients that keep the bacteria alive. Several microorganisms, as an early step in developing a biofilm, form clusters of planktonic/free cells in water. Attachment, cell-to-cell adhesion, expansion maturation, and dispersal are all steps in the biofilm formation process. Microcolonies are formed when bacteria multiply in large numbers are protected from the environment by a coating of hydrogel that traps microbes inside.

Bacterial cells communicate with one another through chemical signals sent by quorum sensing (QS) systems. Cellular activities, population density-based diseases, nutrient uptake, genetic material transfer between cells, motility, and secondary metabolite production all require coordinated cellular communication to function properly. The expansion of the biofilm is similar to that of the EPS. The last stage involves the separation of individual bacterial strains from their microcolonies, which can lead to the establishment of a new biofilm colony elsewhere (Preda & Săndulescu, 2019). And at some point during their time spent in a biofilm, bacteria can shed the structure and resume their planktonic lifestyle. Many internal and external influences are at play here. If sunlight is one among them, that question will be explored here. The figure below depicts the stages of biofilm development.

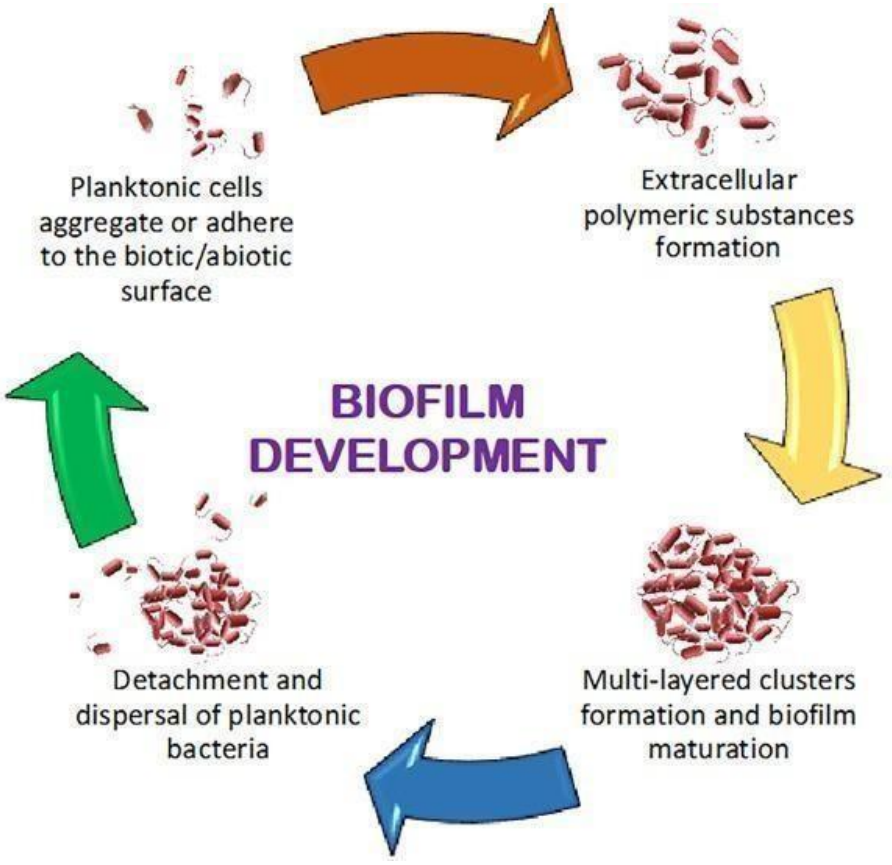

Figure 2.1: Biofilm development cycle (Preda & Săndulescu, 2019)

When bacteria in a certain environment start interacting and bonding with one another, a biofilm is formed. Over time, these networks form into clusters of cells. The biofilm matrix then completely encloses these clumps of cells.

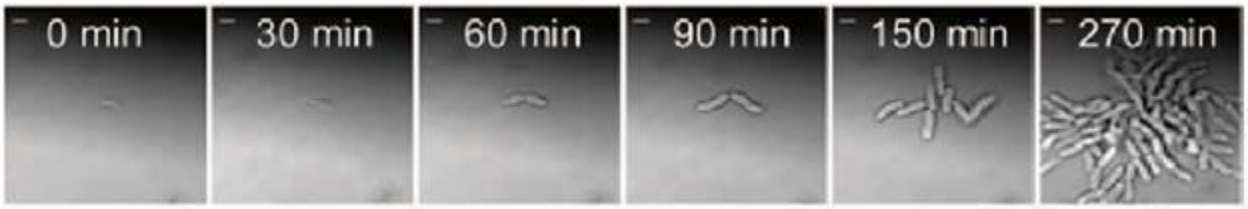

Figure 2.2: Vibrio cell cluster formation (Berk et al., 2012)

Vibrio polysaccharide (VPS) secretion functions as a "glue" or adhesive, bringing *V.cholerae* cells closer together as biofilm maturation progresses, forming the clusters of cells seen above. This causes clusters of vibrio cells to develop into tiny communities called microcolonies.

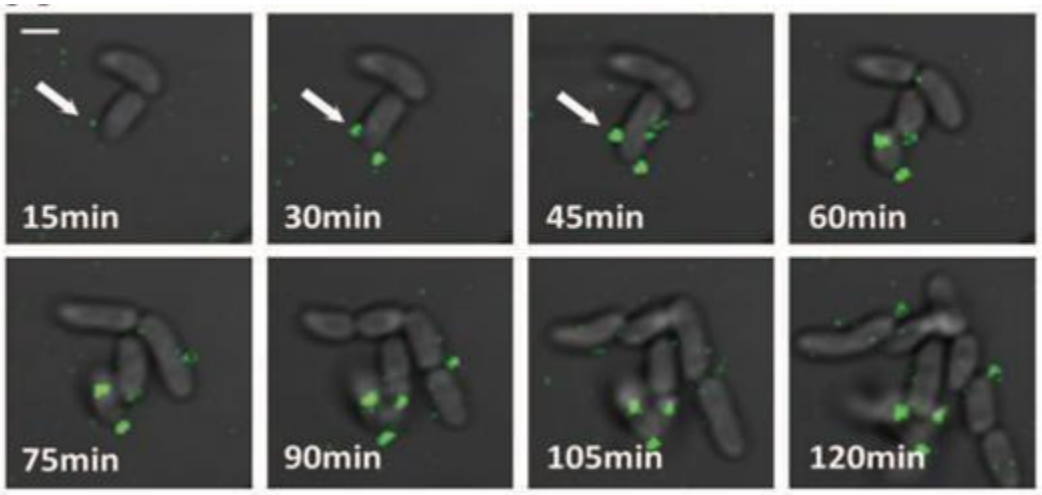

Figure 2.3: **Timelapse image of VPS secretion resulting in vibrio cell cluster**; the green dots represent VPS which is shown to increase in concentration over time (Berk et al., 2012)

The process by which bacteria creates and adheres its biofilm to a solid surface is seen below; in our experiment, we created bacterial biofilm in solid surfaces like glass and plastic.

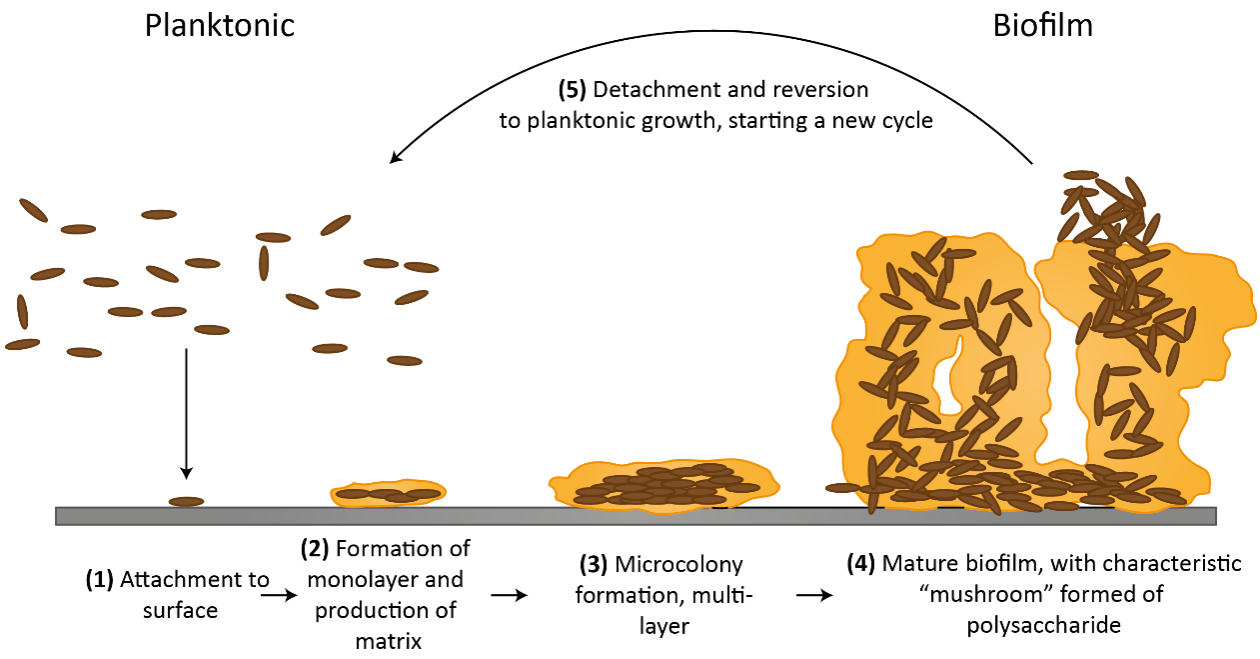

Figure 2.4: **Schematic representation of a biofilm formation on solid surface.** First, the planktonic cells, seen here as brown ovals, attach reversibly to the surface, followed by the adherence to the surface, depicted here in gray (1). The bacteria subsequently produce an extracellular matrix (2), allowing them to form a monolayer and become permanently attached. Then, at the site of the multilayers, a microcolony forms (3). Later on, after the biofilm has fully developed, it forms its signature "mushroom" structures from the polysaccharides (4).

2.2.1 Quorum Sensing and Autoinducers:

Biofilm development, virulence factor expression, secondary metabolite production, and stress adaptation mechanisms like bacterial competition systems, including secretion systems (SS), are all regulated by quorum sensing (QS), a bacterial communication mechanism. The method relies on the chemical signals used by bacteria for intercellular communication in order to measure cell density (Pena et al., 2019). As a result of this communication, the bacterial cells in a dense colony can regulate the gene regulation of each other. Autoinducers are extracellular signal molecules that bacteria produce, release, and then detect to regulate their gene expression in response to cell density. Attaining the autoinducer concentration modifies the expression of target genes, resulting in alterations in behavior that mirror fluctuations in cell number. It has been suggested that in natural environments, bacteria may be able to tell individual species apart within a consortium by their ability to recognize and respond to

different autoinducer signals (Hammer & Bassler, 2003). Since it is believed that bacteria use quorum sensing to coordinate collective behaviors in order to accomplish tasks that would be difficult for an individual bacterium to accomplish alone, it is likely that all of the bacteria in a community or colony communicate in order to collectively express the genes involved in making the biofilm structure.

2.2.2 Quorum Sensing and Biofilm Formation in *Vibrio cholerae:*

Multiple quorum-sensing circuits in Vibrio cholerae cooperate to control virulence and biofilm formation. Because the reaction cascade is dependent on the availability of autoinducers, which are cell signaling molecules, biofilm formation is highly sensitive to differences in cell density. Biofilm formation at low cell densities by *V. cholerae* occurs in the absence of QS autoinducers. Increased concentrations of autoinducers at high cell densities suppress biofilm formation and promote dispersal. Autoinducer-1 (AI-2) and cholerae autoinducer-1 (CAI-1) are the two main autoinducers responsible for this relay operon system; AI-2 is for interspecies communication as it is produced by a wide range of bacterial species, and it is thought that *V.cholerae* uses the AI-2 system to assess the total bacterial cell density in the community (Hammer & Bassler, 2003). There is a common signal relay channel between the two autoinducer systems, which triggers a phosphorelay cascade (Bridges & Bassler, 2019). Both the sensor CqsS, a two-domain protein containing the sensor domain and the histidine kinase domain, and the synthase CqsA, which synthesizes the CAI-1 autoinducer, make up the CAI-1 system. The biofilm is formed when the sensor domain attaches to CAI-1 and the histidine kinase domain phosphorylates LuxO through a phosphorelay cascade (Hammer & Bassler, 2003). Vibrio cholerae requires vibrio polysaccharide (vps) gene clusters, of which VpsA and VpsL are components (Fong et al., 2010). The AI-2 system includes LuxS synthase, which produces the AI-2 autoinducer, and the LuxP/Q sensor, which detects the autoinducer.

signaling molecule and activates the LuxQ protein, a two-domain protein with a sensor domain that interacts with LuxP and a histidine kinase domain that phosphorylates LuxO, setting in motion a chain reaction that culminates in the expression of the vpsA and vpsL genes and the formation of biofilm (Bridges & Bassler, 2019). The overall chain reaction is depicted in the diagram below:

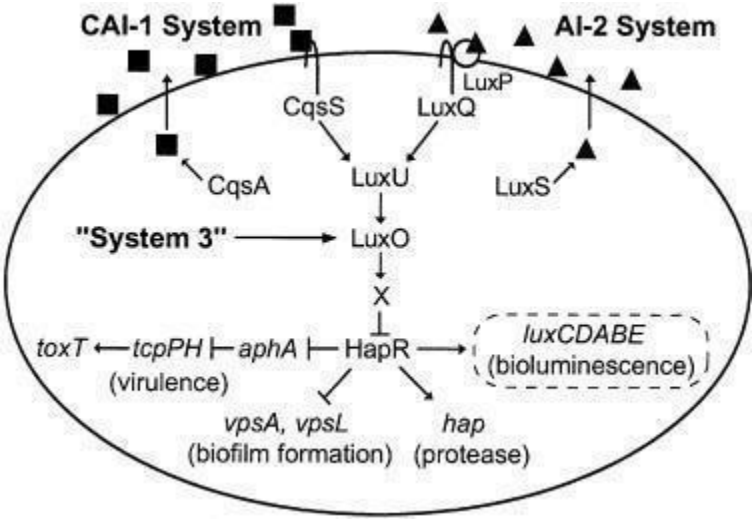

Figure 2.5: Lux operon containing CAI-1 and AI-2 systems involved in biofilm formation in *V.cholerae* due to quorum sensing (Hammer & Bassler, 2003)

Histidine kinase domains of CqsS and LuxQ proteins phosphorylate an integrator protein called LuxU, which in turn phosphorylates the LuxO protein, as depicted above. A repressor gene X is activated when phosphorylated LuxO binds to and interacts with 54. The repressor acts to decrease hapR transcription. By promoting hap protease synthesis while suppressing virulence factors VpsA and VpsL, HapR inhibits biofilm formation. This phosphorelay cascade depends totally on the cell density ((Hammer & Bassler, 2003).

Low Cell Density (LCD):

When autoinducer concentrations are low, phosphate flows from the CqsS and LuxP/Q sensors to the LuxU integrator protein. To get the phosphate to LuxO, LuxU acts as an intermediary. By interacting with 54 (the V. harveyi luxR homologue), phospho-LuxO activates a putative regulator (X) that inhibits hapR production. Some of HapR's target genes are turned on while others are turned off. V. cholerae produces aphA-dependent virulence genes that enhance CT toxin synthesis (Hammer & Bassler, 2003), and biofilm growth occurs at low cell density (i.e., when hapR expression is repressed). The diagram below shows this in action:

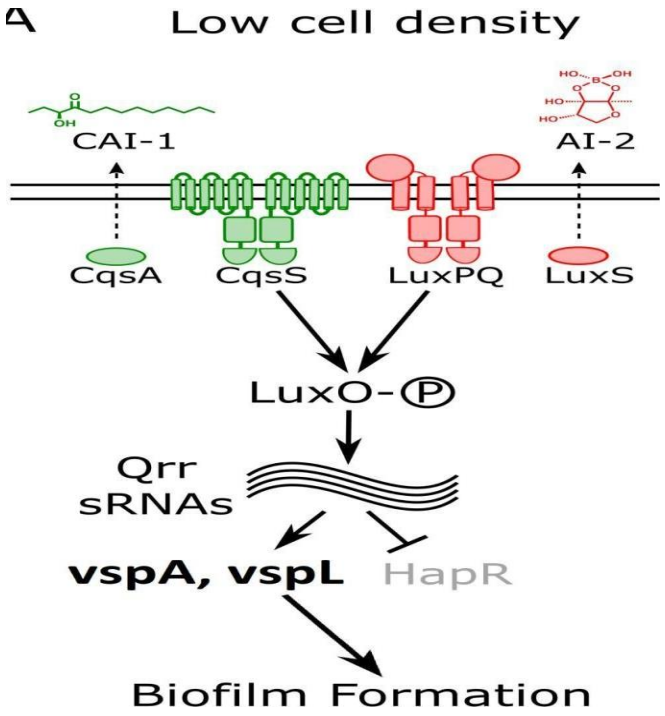

Figure 2.6: Lux operon cascade working at low cell density where hapR is repressed and vspA and vspL are activated so that biofilm is formed (Bridges & Bassler, 2019)

High Cell Density:

At high cell density, the phosphate stream is reversed, leading to dephosphorylation and inactivation of LuxO. By binding to the aphA promoter and inhibiting alphA transcription, HapR inhibits virulence expression and prevents biofilm formation. The mechanism by which this is accomplished is unknown. Furthermore, HapR initiates hap gene transcription, leading to HA/protease production. Because LuxO is not turned on, neither vspA nor vspL are turned on (Hammer & Bassler, 2003).

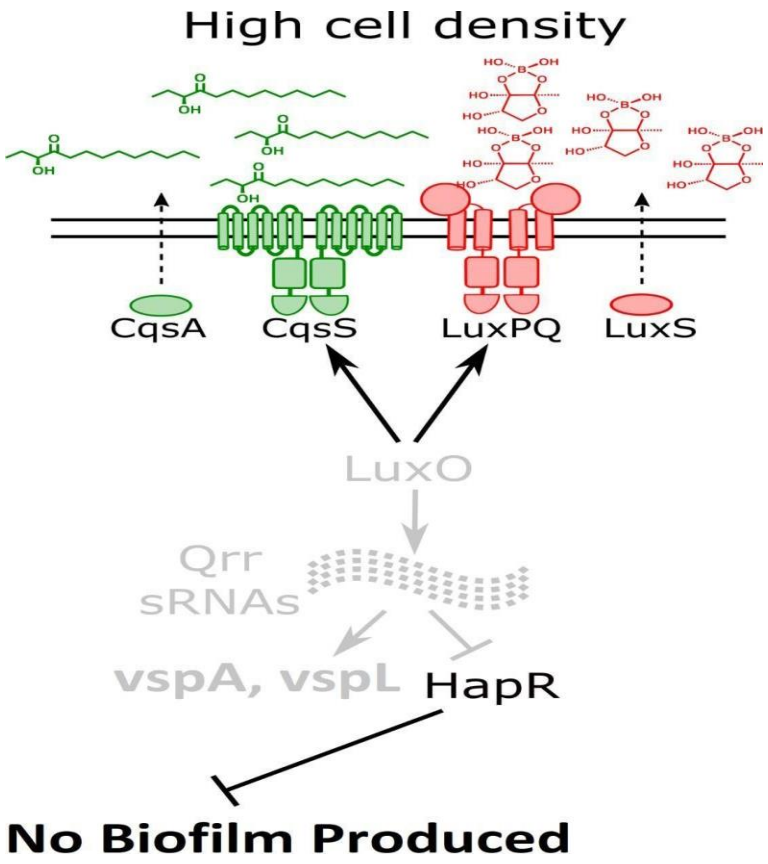

Figure 2.7: Lux operon cascade working at high cell density where HapR is not repressed while vspA and vspL is not activated so that biofilm is not produced (Bridges & Bassler, 2019)

2.2.3 Quorum Sensing and Biofilm Formation in *STEC*:

In *Escherichia coli*, autoinducer 2 (AI-2) uptake is regulated by the LsrABCD transporter complex, its repressor LsrR, and a cognate signal kinase, LsrK. The AI-2 QS system is mainly on this network for quorum sensing. In humans, the entire phosphorelay cascade is located in the lsr operon, where lsr stands for lipolysis-stimulated lipoprotein receptor ("LSR - Lipolysis- stimulated lipoprotein receptor - Homo sapiens (Human) - LSR gene & protein", 2006). Fast uptake of AI-2 is not triggered by high cell density and low AI-2 levels. As a repressor, LsrR binds to and inhibits the expression of numerous genes, including the lsr, flu, and wza genes. There is a lack of biofilm formation at this time because wza and flu are biofilm building proteins (Li et al., 2007). While flu is an autotransporter and a self-recognizing adhesin that is important for biofilm formation in E. coli, Wza is a lipoprotein and an

essential element of the EPS that are the building blocks of E. coli biofilm (Dong et al., 2006). Because phospho-AI-2 derepresses Lsr-mediated AI-2 uptake, it remains suppressed and no AI-2 is uptaken when it accumulates extracellularly during LCD and then either is delivered into cells via a non-Lsr route or accumulates within cells where it binds to LsrR and derepresses several QS genes including lsrR, flu, wza, and dsrA and biofilm is formed. Last but not least, when cellular nutrition is low and AI-2 concentrations reach a "threshold" for absorption, lsr rapidly imports AI-2. Once the imported AI-2 signal is phosphorylated by the cells, LsrR/AI-2 regulation ceases and LsrR/phopho-AI-2 regulation increases. As a result, a shift in the phosphorylation state of AI-2 and its binding to LsrR implies a rapid QS flip (Li et al., 2007). The following diagram shows this in detail:

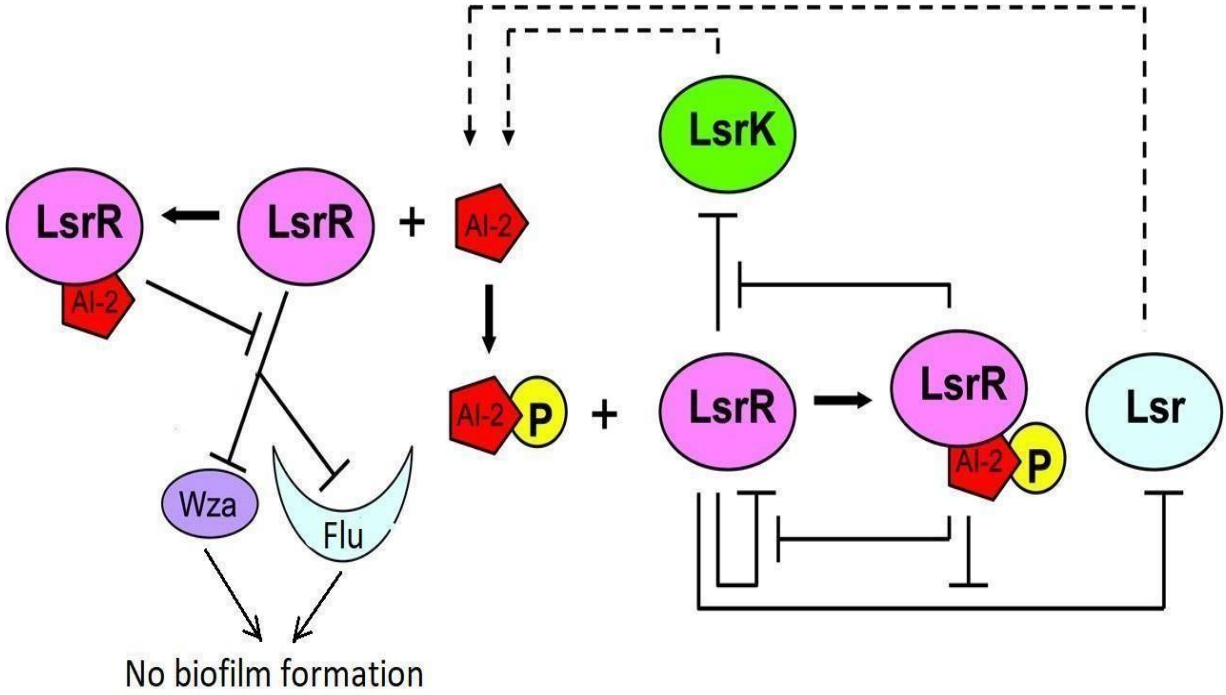

Figure 2.8: Lsr operon in E.coli quorum sensing resulting in Wza and Flu repression and no biofilm formation (Li et al., 2007)

2.4 Mutated *V.cholerae* Strains:

In order to more clearly see how the biofilm breaks down when exposed to sunlight, the *V. cholerae* strains employed in this study are mutant strains "designed" to produce higher amounts of biofilm development. The strains used were *V. cholerae* 1712, a LuxO- mutant created by inserting the LuxO gene into an environmental V. cholerae strain that lacked this gene. This was accomplished using a plasmid called pLuxO. On the other hand, *V. cholerae* 1877, a mutant strain of the bacteria, was employed. To maintain the production of VPS and thus biofilm, the Lux operon is kept active in this HapR mutant strain by constantly repressing the HapR gene.

2.5 Pathogenic Significances of Biofilms:

Now widespread in the environment, biofilms can be found anywhere from sewage treatment plants to food processing plants to sensitive medical devices (Mosharraf et al., 2020). The NIH estimates that biofilms are responsible for 80% of all human illnesses. Many pathogenic bacteria, the kind that can make people sick, create biofilms. In fact, in order to cause severe sickness, some of them must go from being sessile to being motile. The bacterium Vibrio cholerae can switch between a motile and biofilm form. Over the past few decades, researchers have made great strides in their ability to predict, manage, and utilize biofilms created in the lab. There is some evidence that during infection, Vibrio cholerae can form biofilm-like aggregates, which may play an important role in disease pathogenesis and transmission. This bacterium is highly mobile, allowing it to invade its target environment and establish a firm foothold, while the biofilm condition offers the necessary host resistance. A pathogen needs to colonize the human intestine, spread throughout the body, and be expelled in order to create an illness. The virus moves throughout the human stomach in this manner. Pathogens pump harmful CT Toxin into intestinal cells after binding to them. Patients with cholera excrete a mixture of slime, cluster, and single cholera cells in their feces. The research was done by Silva and Benitez (2016). This results in the spread of the cholera bacterium from one individual to the next.

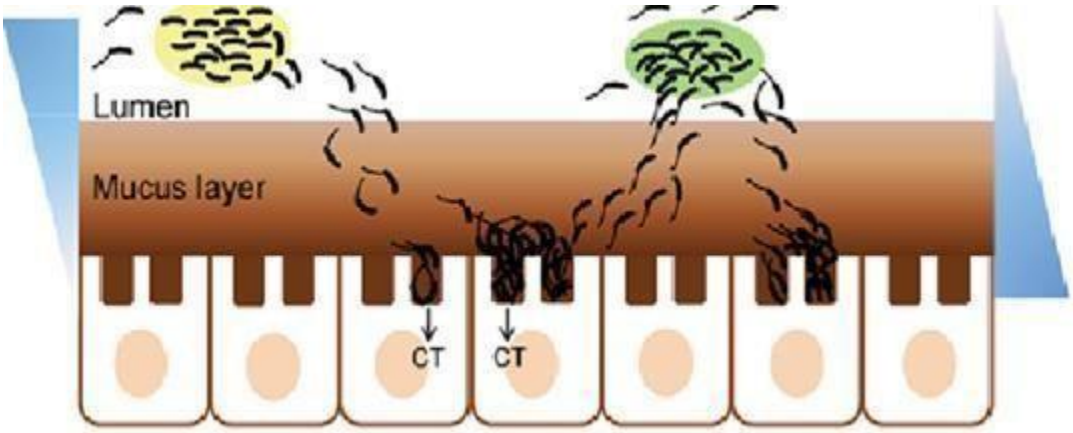

Figure 2.9: Transitions of *vibrio cholera* between sessile and motile form (Silva & Benitez, 2016).

In addition to forming biofilms in environmental circumstances and on plants, *STEC* is also capable of doing so on a wide variety of surfaces commonly seen in meat processing plants, such as stainless steel, polystyrene, glass, polyurethane, and high-density polyethylene. When contaminated food is brought into processing facilities, *STEC* is able to spread and contaminate other foods..

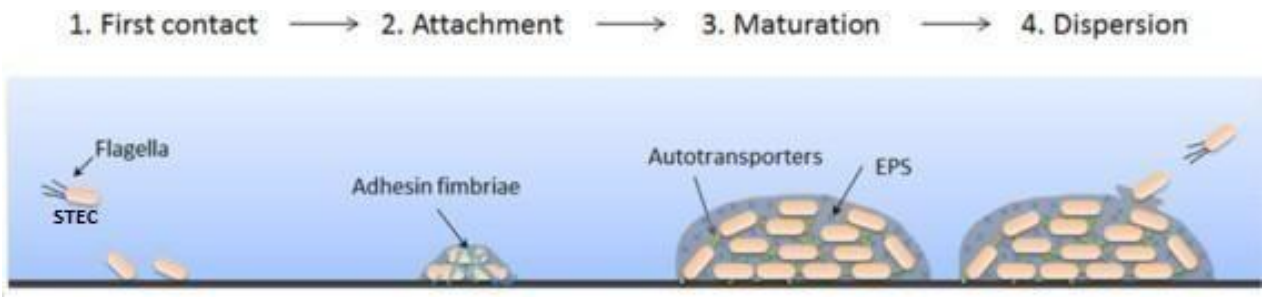

Figure 2.10: Schematic representation of biofilm formation in STEC on surfaces like solid environmental surfaces or gut linings (Vogeleer et al., 2014)

2.6.1 Diseases Caused by *V.cholerae*:

Humans infected with *Vibrio cholerae* experience watery diarrhea, vomiting, and dehydration due to the disease cholera. Cholera pathogenesis follows a fairly precise route, with the bacterium entering the human body through polluted water. Once within the small intestine, where it will reside for the foreseeable future, *Vibrio cholerae* will begin expressing virulence factors including cholera toxin. The CtxB pentameric subunit of cholera toxin attaches to the ganglioside GM1 on the cell membrane. CtxA and CtxB are the two subunits that make up the whole toxin. The cholera toxin that has been attached to

GM1 is then taken up by the cell and transported to the ER. This leads to the dissociation of the CtxA and CtxB components. CtxA is an enzyme subunit. ADP ribosylation factor 6 (ARF6) is allosterically activated when it is released from the endoplasmic reticulum (ER) into the cytoplasm. The ARF6-CtxA complex catalyzes adenylyl cyclase, a G protein-coupled receptor. Cystic fibrosis transmembrane receptor (CFTR) is phosphorylated (P) (phosphorylated) when cAMP levels rise in the cell. Because of this, watery diarrhea develops because ions and water are effluxed into the small intestinal lumen (Baker-Austin, 2018).

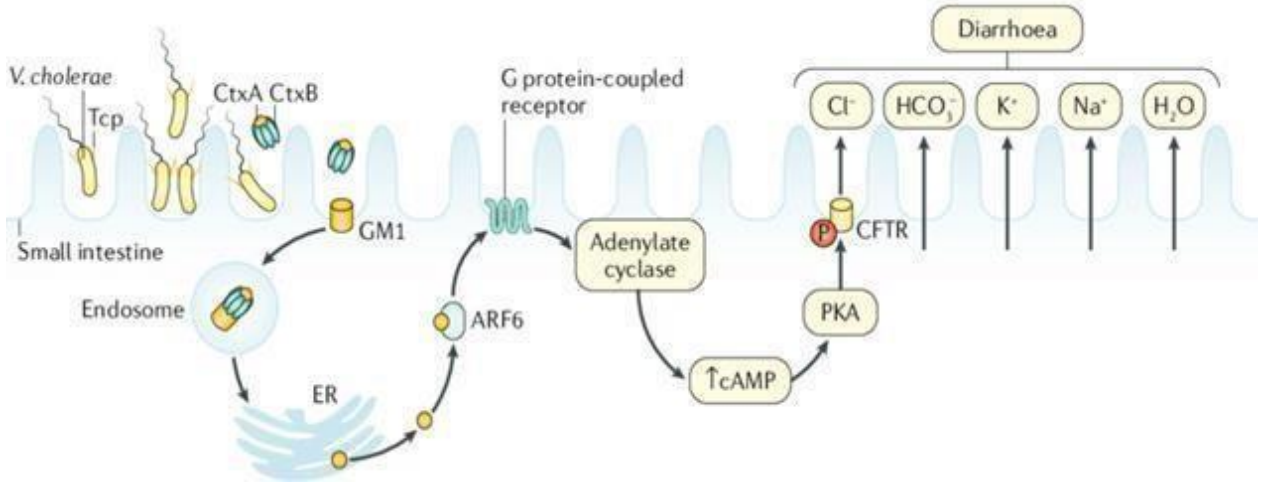

Figure 2.11: Cholera Pathogenesis (Baker-Austin, 2018)

2.6.2 Diseases Caused by *STEC*:

Shiga toxin-producing Escherichia coli (STEC) are pathogenic bacteria found in food that, in humans, can damage the intestinal mucosa and, in rare cases, other internal organs. E. coli O157 is the offending microorganism. Most often documented adherence systems include the adhering and effacing (A/E) lesions of enteropathogenic *E. coli* with the intimin gene (eae) and the fimbria of enteroaggregative *E. coli*. Enterohemorrhagic disorders are caused by these microorganisms when they attach to the intestinal lining and express Shiga toxin (HUS) (Nastasijevic et al., 2020). HC and HUS are both potentially fatal conditions. Fever, diarrhea, and vomiting are all indications of a *STEC* infection. Most patients make a full recovery by day 10, and the incubation period for this organism is only 3 to 8 days. The optimal temperature for *STEC* growth is 37 degrees Celsius, however it may survive in temperatures as low as 7 degrees Celsius. However, if the bacteria are in their biofilm stage, they can survive at greater distances. Temperatures between 7°C to 50°C. Meals with an aW of 0.95 or lower and foods with a pH of 4.4 or below are both conducive to the growth of *STEC*. It can be

eliminated by cooking food to a temperature of 70 degrees Celsius or higher throughout. Serotypes of enterotoxigenic *Escherichia coli* (*STEC*) other than *E. coli* O157:H7 have been linked to isolated cases and outbreaks in recent years ("*E. coli*", 2018). In addition, the *STEC* are less susceptible to sanitizers and disinfectants while they are in their mobile biofilm stage, making it more difficult to kill them (Vogeleer et al., 2014). After ingestion, the bacteria may attach to Peyer's patches and the follicle-associated epithelium of the terminal ileum. Colonization is aided by quorum sensing and activation by the host hormonal response during hemorrhagic colitis, which presumably involves adrenaline and norepinephrine. Paneth cells' globotriaosylceramide Gb3 receptor is a key player in Shiga toxin's translocation across the intestinal epithelium. The toxin has been shown to trigger intestinal apoptosis and dysentery. Intestinal bacteria are eliminated by the inflammatory host response. When the gut immune system is weakened, more bacteria are able to grow and spread their virulent genes throughout the body (Karpman, 2012).

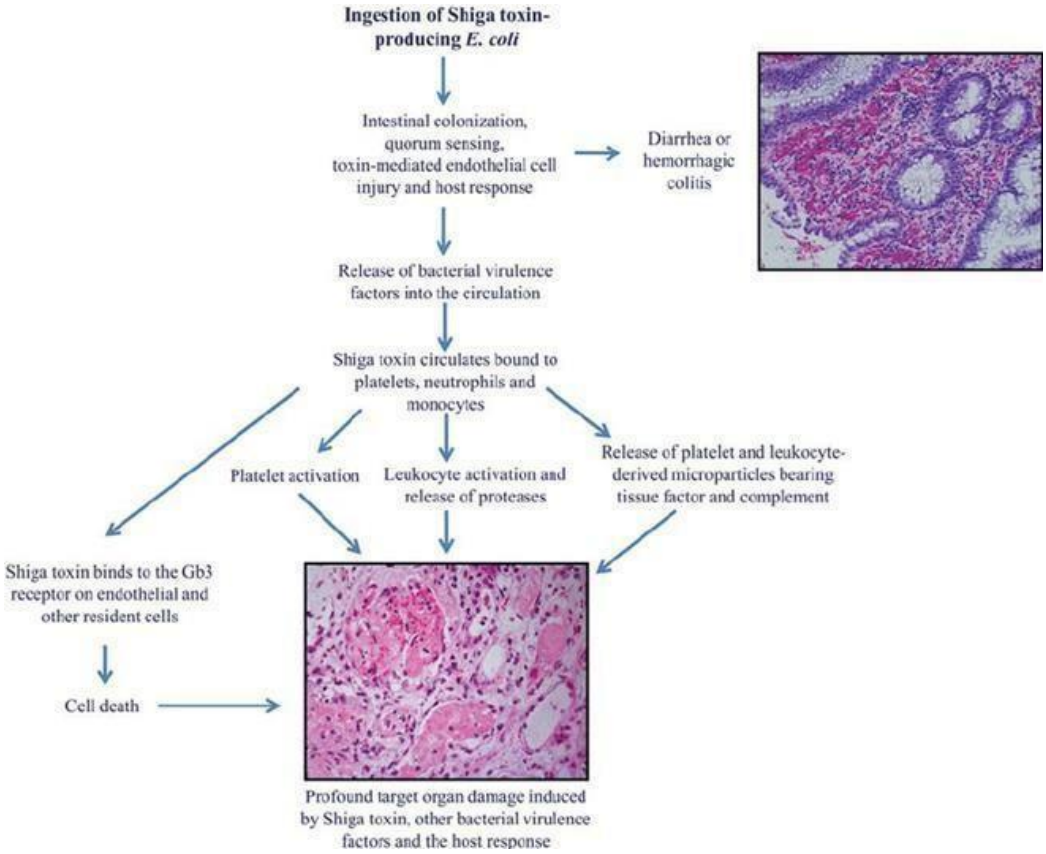

Figure 2.12: Pathogenesis of *STEC* (Karpman, 2012)

2.7 Biofilm and diseases:

Compared to their planktonic counterparts, biofilm producing microorganisms have different characteristics like resistance to host defenses, antibiotics treatment and unique growth rates. This resistance to host defenses is caused by the production of antibodies that cannot penetrate the biofilm surface. Besides, although antimicrobial treatment might initially have an effect, after completion of the antibiotic therapy frequent relapses occur as bacteria inside the biofilm remain unaffected due to incomplete antimicrobial penetration. In addition, within a biofilm bacteria can transfer extrachromosomal genetic elements- resistance plasmids, further causing resistance in bacteria. Biofilm-related infections are frequently caused by *Staphylococcus epidermidis, Gardnerella vaginalis, Candida albicans, Pseudomonas aeruginosa, Klebsiella pneumoniae* and *Enterococcus faecalis* etc (Del Pozo, 2018).

2.8 Cholera Biofilm and epidemics:

Around 1,200 cholera patients from various locations were admitted to hospitals in Dhaka city in March 2022, the majority of which were operated by the International Centre for Diarrheal Disease Research, Bangladesh (icddr,b). This year, the number of patients was more than typical, as the hospital administration reported each day almost a thousand of patients arrived complaining about diarrhea and cholera ("Dhaka Wasa must answer for cholera outbreak", 2022).

Cholera outbreaks and pandemics are a major health problem in many nations across Asia, Africa, and Latin America due to the two *V. cholerae* serotypes O1 and O139 (Alam et al., 2007). Cholera outbreaks in Bangladesh typically occur between March and May and again between September and October, indicating a seasonal cycle of *V. cholerae* (Faruque et al., 2005). Isolation of aggregation of *Vibrio cholerae* from cholera stool revealed the presence of biofilm fragments during cholera epidemics. These cells were first found to be infective and culpable, but their infectivity rapidly declined, suggesting a time limit on their infectious potential. As a result, in regions with inadequate sewage treatment systems, these cells can only exacerbate cholera epidemics (Alam et al., 2007). So, the mystery persists: why do cholera epidemics seem to occur every year around the same time?

Biofilms of nonculturable V. cholerae O1 cells that can only be spotted using fluorescent antibody research persist in aquatic environments in Bangladesh all year long. This annual cycle and epidemics of cholera can be explained by the fact that cells originating from these biofilms can be made culturable even after a year of slumber. Changes in temperature, nutrition levels, and the summer bloom of zooplankton (the host of *V. cholerae*) are typically thought to be the root causes of the resurgence of *V. cholerae* in nature. Biofilms, but not nonculturable microcosms, were responsible for the resuscitation (Alam et al., 2007). During epidemics, water samples contained both free-floating and biofilm-bound *V. cholerae* O1 that could be cultured; however, these cells remained nonculturable the rest of the year and served as a reservoir for the yearly recurrence of the disease (Sultana et al., 2018).

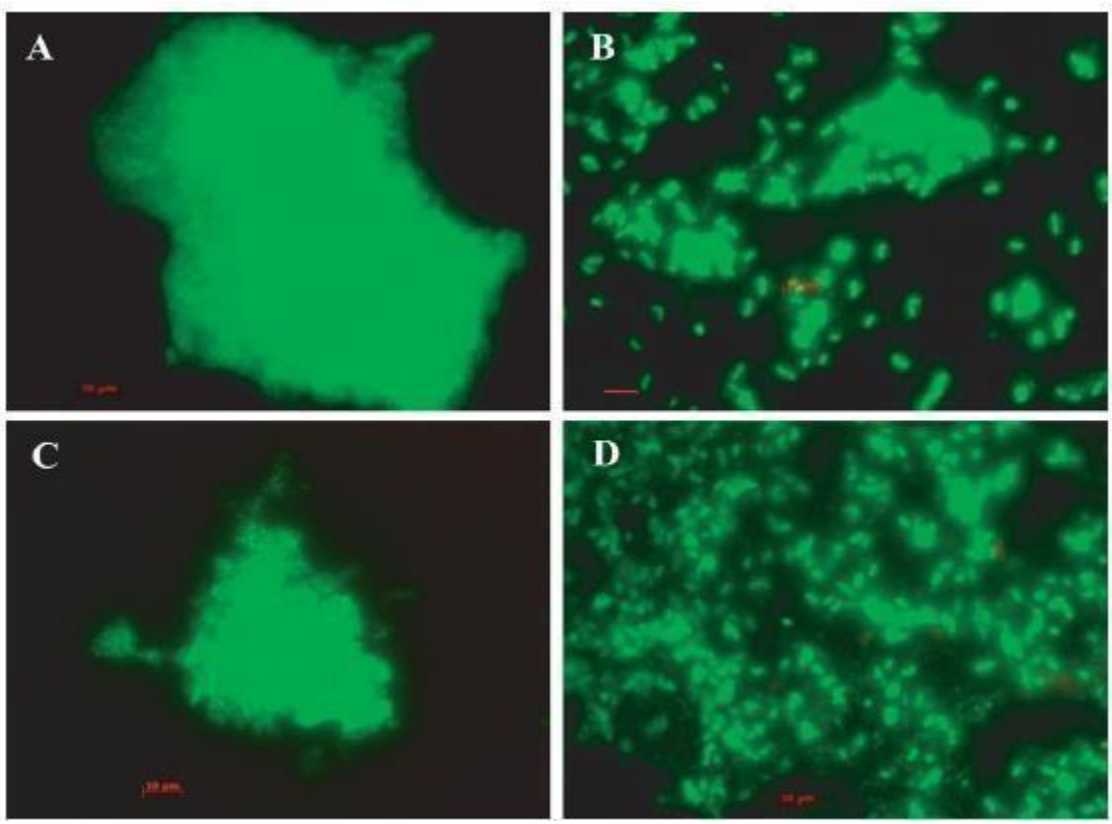

Figure 2.13: *V. cholerae* O1 is detected in the Bay of Bengal's aquatic ecosystem using direct fluorescent monoclonal antibody (DFA). This detection reveals biofilms of the bacteria during the winter and monsoon months (A and C) and free-living *V. cholerae* O1 cells during the spring and fall months (B and D). (Sultana and others, 2018).

2.9 ELISA

In this investigation, an enzyme-linked immunosorbent assay (ELISA) was used to determine the optical density (OD). A useful method for determining a biofilm's OD is the micro-ELISA auto-reader approach (Mosharraf et al., 2020).

ELISA is a commonly employed technique in nearly all immunology laboratories. The concept of antigen-antibody interaction governs this. The OD can then be measured using ELISA Auto reader equipment to quantify this interaction. With ELISA, substances such as proteins, peptides, hormones, and antibodies can be recognized and quantified.. ELISA comes in three primary varieties, though. Those are:

- Direct ELISA
- Indirect ELISA
- Sandwich ELISA

All these methods were not applied in this experiment. To determine the OD of the biofilms that had developed inside of ELISA plates, only the ELISA Auto reader's OD measurement feature was utilized.

2.10 Coomassie Stain and Dissolving Coomassie Stain with Glacial Acetic Acid

An example of a disulfonated triphenylmethane dye is Coomassie Brilliant Blue G-250. Their primary function is to color proteins when they bind to protonated basic amino acids via hydrophobic interactions with aromatic residues and electrostatic contact with lysine, arginine, and histidine. They do not obstruct the mass spectrophotometry of the dyed biofilm rings since the CBB G-250 dye is reversible and non-covalent (Steinberg, 2009). The CBB G-250 dyes the aforementioned biofilms based on the extracellular proteins released by the contained bacteria, the extracellular matrix proteins found in VPS, and the adhesins, pili, and flagella that make up a typical biofilm structure. Along with the extracellular chitin-binding protein GbpA, which is utilized to mediate the attachment of the biofilm structure to a zooplankton's chitinous surfaces, three of the primary proteins found in the VPS are RbmA, Bap1, and RbmC, all of which are crucial for biofilm formation (Fong, 2015). These proteins are therefore the target biofilm components that the CBB G-250 uses for the study's coloring and imaging. When proteins bind to CBB G-250 in an acidic environment, their positive charges keep the protein from protonating, giving the protein a blue hue. When a protein binds to the dye, its maximum absorption shifts from 465 to 595 nm. Phase 2 of the study measures this increase in absorbance at 595 nm, which will be covered in more detail later in the paper (Roger, 2017). 33% glacial acetic acid can be used to solubilize Coomassie stains that are attached to the biofilm (Stepanović et al., 2000).

Chapter3: Materials And Methods

3. Materials and Methods:

3.1 Organisms:

4 strains of bacteria were used. These are:

1. *Shiga toxin-producing Escherichia coli (STEC)*
2. *Vibrio Cholerae 1877* (HapR mutated)
3. *Vibrio Cholerae 1712* (LuxO induced)
4. *Vibrio Cholerae WT324*

3.2.1 Bacterial Culture Media:

In this experiment, LB Agar medium and Luria Broth (LB) were utilized. Gram negative bacteria make up every organism in this environment, and LB is an ideal growth medium for them. In addition, 0.8% LB Agar medium was employed as a preservation medium. Within, bacterial stocks were maintained and coated with paraffin.

Every culture and medium was obtained from BRAC University's Life Science Laboratories. Using accepted practices, they were brought back to life, used, and preserved.

3.2.2 Biochemical Tests

In order to verify the bacterial strains employed in this investigation, several biochemical tests were performed. The vibrio cholera strains were tested on Thiosulfate-citrate-bile salts-sucrose (TCBS) agar media to determine whether or not they were indeed vibrio. The *Vibrio cholerae* strains were verified to be *Vibrio cholerae* if the green TCBS agar turned yellow after streak plating them on the TCBS agar media plate and incubating it at 37°C for 24 hours. If the strains stayed green or any other color, they were considered to be something else. All three *V. cholerae* strains produced yellow colonies following TCBS plating, whereas STEC stayed green.

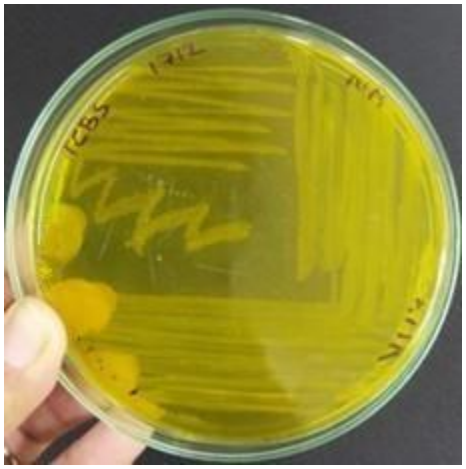

Figure 3.1: *1712 V.cholerae* showing in yellow colonies in TCBS agar plate

Figure 3.2: *STEC* showing green colonies in TCBS agar plate

The *STEC* was tested on triple sugar iron agar (TSI) to verify that it was *E. coli*. *STEC* colonies were removed from a LA plate harboring *STEC* using an inoculation needle. The TSI slant agar was stabbed with a needle, and the same needle was used to streak the slant surface of the agar medium while it was being removed. Following the inoculation, the TSI test tubes were incubated for 24 hours at 37°C. It was determined that the test tubes exhibiting a yellow slant and butt were *STEC*.

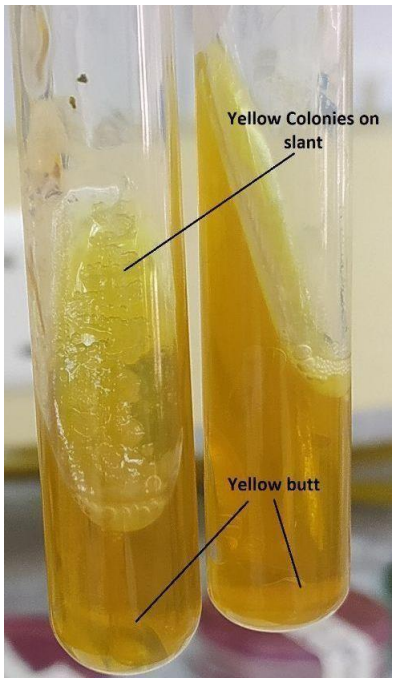

Figure 3.3: *STEC* showing yellow colonies on slant and a yellow butt on TSI media

When streaked and cultured at 37°C for 24 hours, the *STEC* likewise produced yellow colonies in XLD agar media plates, confirming it as an E. coli strain. In order to maintain the appropriate bacterial strains throughout the study, these tests were conducted on a regular basis.

3.3 Overview of the Methods:

Initially, fresh cultures were generated and the strains were brought back to life from the bacterial stocks. After being inoculated with fresh LB, these fresh cultures were kept in the shaker incubator for the entire night. From here, active cultures were made and used to create static biofilms in vials, falcon tubes, and ELISA plates.

Following the formation of biofilms, the samples are separated into two groups, one of which is exposed to sunlight while the other is kept in the dark for the same amount of time. Thereafter, four distinct phases were used to ascertain the biofilms' properties. During these stages, measurements were made of the biofilms' cell count, OD, and OD after staining. Additionally, staining and imaging were used to track changes in the biofilm's thickness over time.

3.4 Revival of Bacterial Culture:

The laboratory stocks that were kept in T1N1 medium were used to resurrect the bacterial strains. The stocks' cultures were brought back to life by creating a subculture on LB agar plates using the streak plate method. Single colonies were isolated from these plates after they were cultured for 24 hours at 37°C.

3.5 Making Young Culture and Biofilm:

Single colonies from the agar plates were taken to inoculate 1 ml LB in eppendorf tubes in order to prepare young culture. To create the overnight culture, this was kept in a shaker incubator for the entire night. After adding 500 µL of the overnight culture to 9.5 ml of fresh LB in test tubes or falcon tubes, the mixture was shaken in an incubator until turbidity was noted. To guarantee biofilm formation, these early cultures were subsequently moved to glass vials, falcon tubes, and ELISA plates and left undisturbed for 72–96 hours. In phase 3, a coverslip was partially submerged when it was placed inside the falcon that held the young culture.

3.6 Discarding Old Culture and Adding New Media

New media was added and the old cultures were disposed of after the biofilm had formed for seventy-two hours. Using micropipette tips, the biofilm layer that had initially developed on top of the culture was carefully scraped from the vials. Next, the biofilm ring on the vial surface was left intact by carefully removing the previous culture with a micropipette. To guarantee that the majority of the bacteria and surface biofilm were removed, the vial/falcon tubes were cleaned twice using sterile LB media. Lastly, more LB was added to the vials, typically 1000 µL, which was sufficient to entirely immerse the coverslips holding the biofilm in falcon tubes and the biofilm rings in vials.

The coverslips were taken out of the old cultures in the falcon tubes after 96 hours of biofilm formation. They were then divided, gently rinsed with sterile saline, and placed into the falcon tubes holding the new LB media. To get rid of the excess layer of biofilm on the cover slip, saline was rinsed over it. The media completely engulfed the coverslips.

3.7 Exposure in Sunlight and Dark

3.7.1 Phase 1: Glass vials

The biofilms in the glass vials were formed over the course of 72 hours and were then subjected to light and dark for 6-hour intervals. There were four vials of each of the four bacterial strains included in each set. One vial from each pair was taken out on day one so that readings could be taken during a period of continuous darkness and zero daylight hours. Three days in a row, the vials were exposed to light and darkness for 6 hours at a time. After each day's exposure, the cultures were plated using the droplet method, and the vials were stained so that the changes in the biofilm rings could be observed.

Figure 3.4: Exposure of glass vials containing bacterial biofilm to sunlight as part of phase 1 data collection.

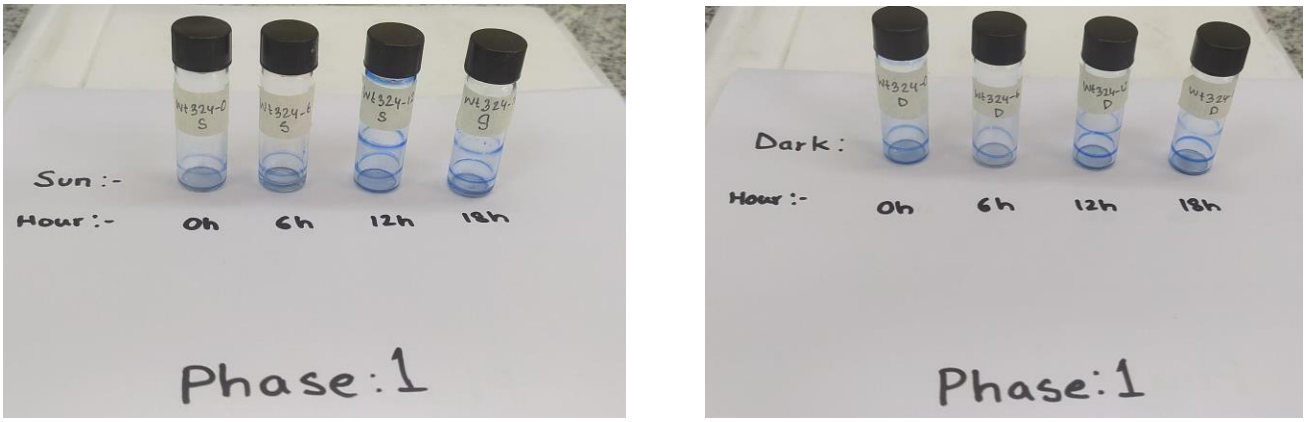

Figure 3.5: The changes in the biofilm ring of *Vibrio WT324* strain due to exposure of sunlight and darkness over a period of 18 hours. The blue rings inside the glass vials are biofilm rings that were stained with CBB G-250 solution overnight and then washed with saline

3.7.2 Phase 2: Optical Density of Dissolved Biofilm Rings

Here, we use glacial acetic acid (33%) to dissolve the CBB G250-stained biofilm rings. The lowest biofilm rings were submerged in glacial acetic acid poured into the vials with a micropipette to dissolve the stain. Glacial acetic acid was carefully poured into vials where a second biofilm had formed following exposure, taking care to avoid the upper ring and dissolve only the lower biofilm ring. The stain dissolves into the solution, turning it blue, once the vials are gently shaken..

Figure 3.6: CBB G-250 stained biofilm ring dissolved by 33% glacial acetic acid forming a blue solution of different blue color spectrum according to the thickness of the biofilm rings used for phase 2 data collectio

3.8 Biofilm Staining and Washing

We used sterile saline (0.9NaCl) to gently wash the vials and coverslips before drying them and staining them with Coomassie Brilliant Blue G-250. After staining the biofilm thoroughly overnight, the excess dye was removed by washing with sterile saline.

Figure 3.8: Coomassie Blue dye prepared to stain the biofilms using CBB G-250 powder

3.9 Dissolving Stained Biofilm Rings

The second step involved rinsing the dyed biofilm rings with sterile saline to get rid of any remaining dye. Glacial acetic acid was then applied to the rings, and the spots vanished instantly. Dissolved and transferred to 96-well ELISA plates, the biofilm ring samples that had been dyed for a week were analyzed for their optical density (OD). The OD measured obvious differences between the biofilm in sunlight and in the dark.

After 6-12 hours, a second biofilm ring had grown in the glass vials. To get the required outcomes, it was necessary to simply disintegrate the outermost ring of the biofilm.

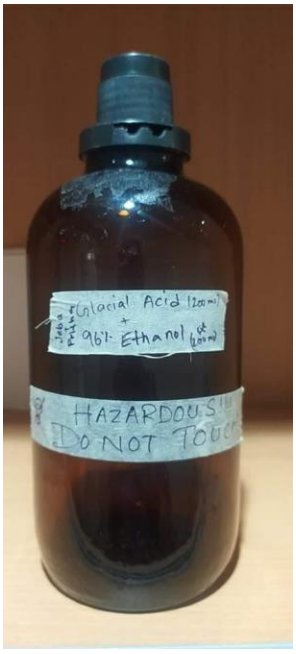

Figure 3.9: 33% glacial acetic acid used to dissolve stained biofilm rings

3.10 ELISA of Biofilm Stains

Glacial acetic acid was used to remove the stains from the biofilm rings that had grown in the vials. After the stain was dissolved, 200 L was added to each well of the 96-well ELISA plate. MultiscanEX ELISA Machine was used to get the result. A replication was stored for every 6 hours to determine the mean OD.

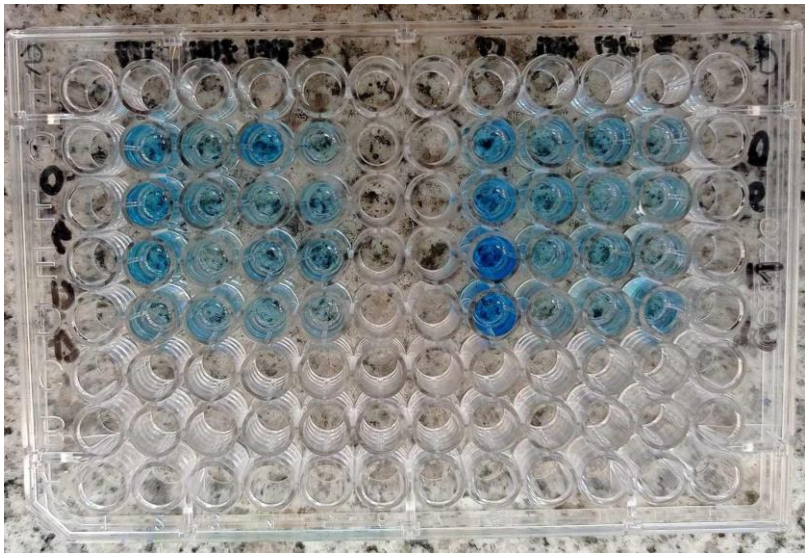

Figure 3.10: **Dissolved biofilm stains in 96 well ELISA plate**. In phase 2, using glacial acetic acid, the stained biofilm rings were dissolved and 200 µL of the dissolved stain solution was used to fill each well of the ELISA plates.

3.11 ELISA of Biofilms

The absorbance of the biofilms was determined using a 450 nm wavelength and a ThermoScientific MultiscanEX ELISA Machine. Every day, readings were taken every two hours. As a negative control, we filled some of the wells with media.

Figure 3.11: MultiscanEX ELISA Machine by Thermo Scientific

3.12 Statistical analyses

Microsoft Excel and IBM SPSS Statistics version 29.0.2.0, analytical software for Windows, were used for statistical analysis. The statistical differences between two groups were examined by independent samples T Test assuming equal variances. The significance level was chosen 0.05 or 95% as a standard. In this research, two-tailed t Tests were performed.

Chapter 4: Results

4.1.1 PHASE 1: Biofilms formed on Glass Plates

a. 

b. 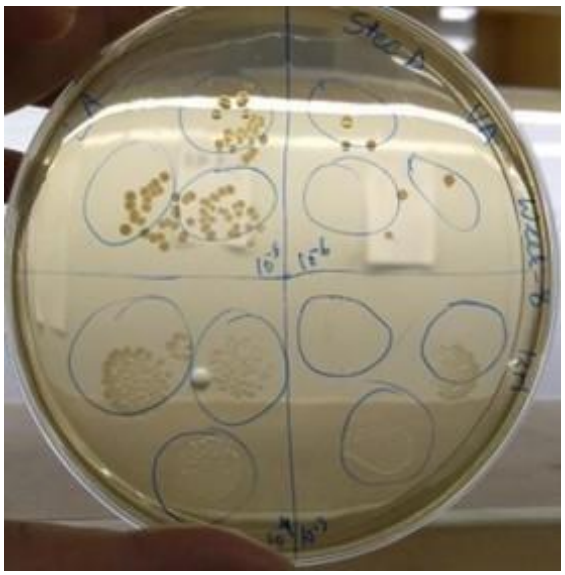

c. 

d. 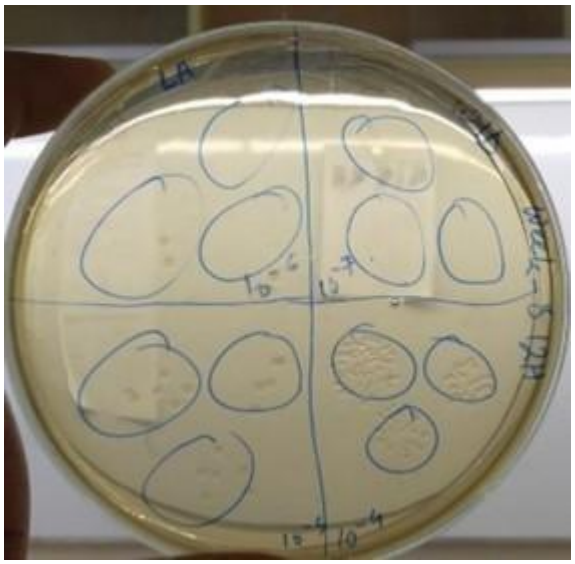

e. 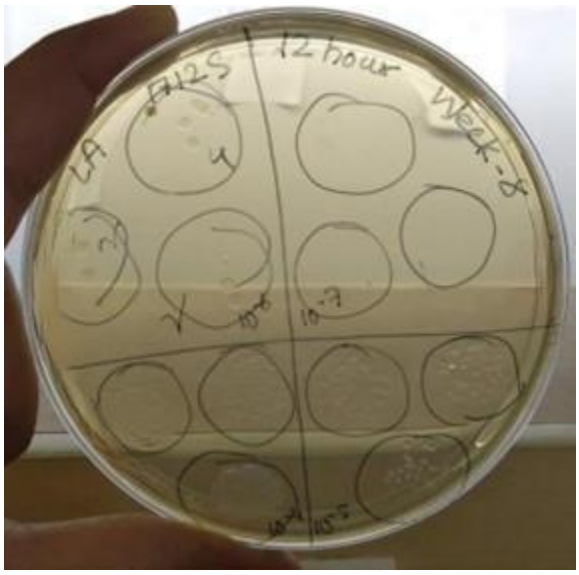

f. 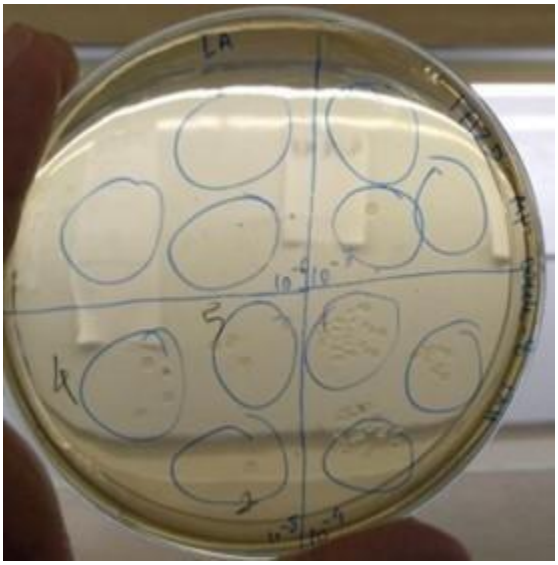

Figure 4.1**: Petri dishes showing the colonies of the respective bacterial strains**. The bacterial colonies on the plates were plated using the droplet method and were diluted by a factor of 104, 105, 106, and 107 over the course of 24 hours. colonies from *STEC* culture after biofilm was exposed to 12 hours of sunlight; colonies from *STEC* culture after biofilm was exposed to 12 hours of darkness; colonies from 1877 Vibrio culture after biofilm was exposed to 12 hours of darkness; colonies from *WT*324 *Vibrio* culture after biofilm was exposed to 12 hours of darkness; colonies from 1712 Vibrio culture after biofilm was exposed to 12 hours of darkness; colonies from 1712 Vibrio culture after biofilm was exposed to 12 hours of darkness; colonies from 17 The dots represent bacterial colonies.

4.1.2 Phase 1 Graphs and Regression Analysis

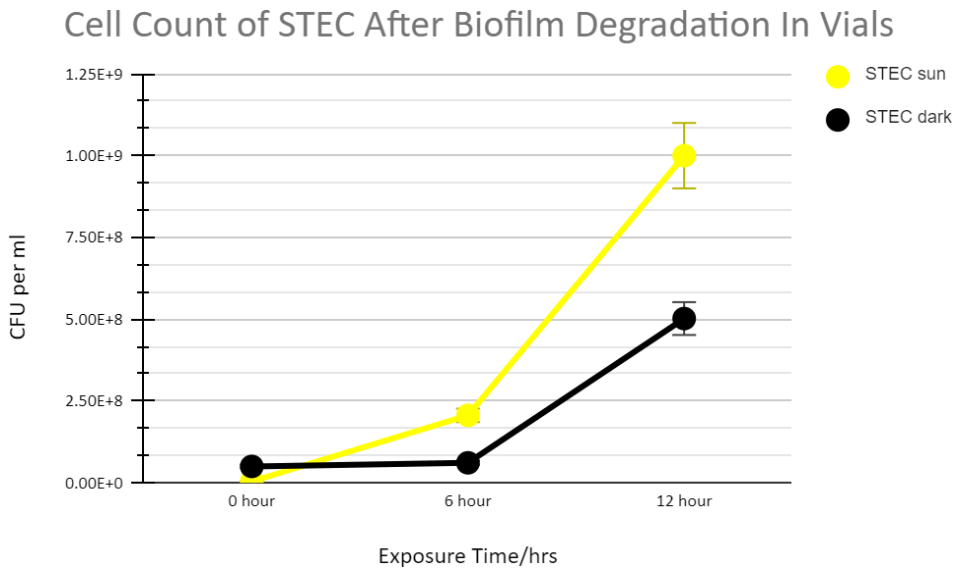

Figure 4.2: Graphical representation of cell count of *STEC* after biofilm degradation in sunlight and in darkness taken from phase 1 data. X axis represents the exposure time in hours and Y axis represents CFU per ml

Organism	R value and interpretation	R^2 value and interpretation	Regression model and interpretation
STEC SUNLIGHT	0.946 Strong positive correlation	R^2= 0.895 89.5% of the total variation of the cell count can be explained by the regression model.	y=-9.47E+07 + 8.3E+07*x On an average, when the time of exposure in sunlight is 0 hour, the cell count is 9.47E+07 CFU/ml and when the time of exposure increases by 1 hour, cell count increases by 8.3E+07 CFU/ml.
STEC DARK	0.876 strong positive correlation	R^2= 0.768 76.8% of the total variation of cell count can be explained by the regression model.	y=-2.17E+07 + 3.77E+07*x On average, when the time of exposure in the dark is 0 hour, the cell count is 2.17E+07 CFU/ml and when the time of exposure increases by 1 hour, cell count increases by 3.77E+07 CFU/ml.

Table 1: R value, R square value, regression model and their respective interpretations for *STEC* exposed to winter sunlight and darkness taken from phase 1 data

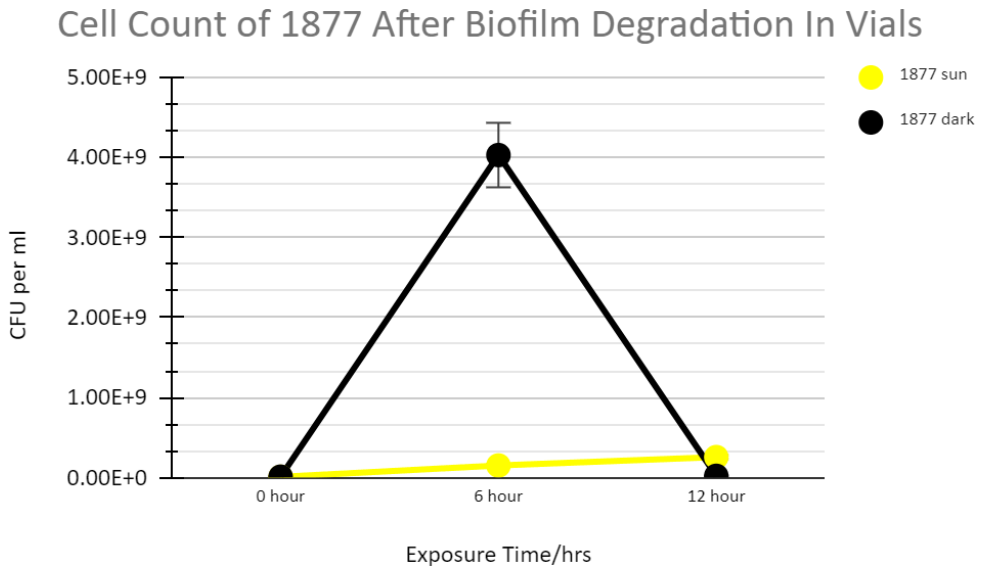

Figure 4.3: Graphical representation of cell count of *Vibrio 1877* after biofilm degradation in sunlight and in darkness taken from phase 1 data. X axis represents the exposure time in hours and Y axis represents CFU per ml

Organism	**R value and interpretation**	**R^2 value and interpretation**	**Regression model and interpretation**
1877 SUNLIGHT	0.996 Strong positive correlation	R^2= 0.993 99.3% of the total variation of the cell count can be explained by the regression model.	y=1.42E+07 + 2.06E+07*x On average, when the time of exposure in sunlight is 0 hour, the cell count is 1.42E+07 CFU/ml and when the time of exposure increases by 1 hour, cell count increases by 2.06E+07 CFU/ml.
1877 DARK	0.002 Weak positive correlation	R^2= 0.000004 0.0004% of the total variation of cell count can be explained by the regression model.	y=1.35E+09 + 8.75E+05*x On average, when the time of exposure in dark is 0 hour, the cell count is 1.35E+09 CFU/ml and when the time of exposure increases by 1 hour, cell count increases by 8.75E+05 CFU/ml.

Table 2: R value, R square value, regression model and their respective interpretations for *Vibrio 1877* exposed to winter sunlight and darkness taken from phase 1 data

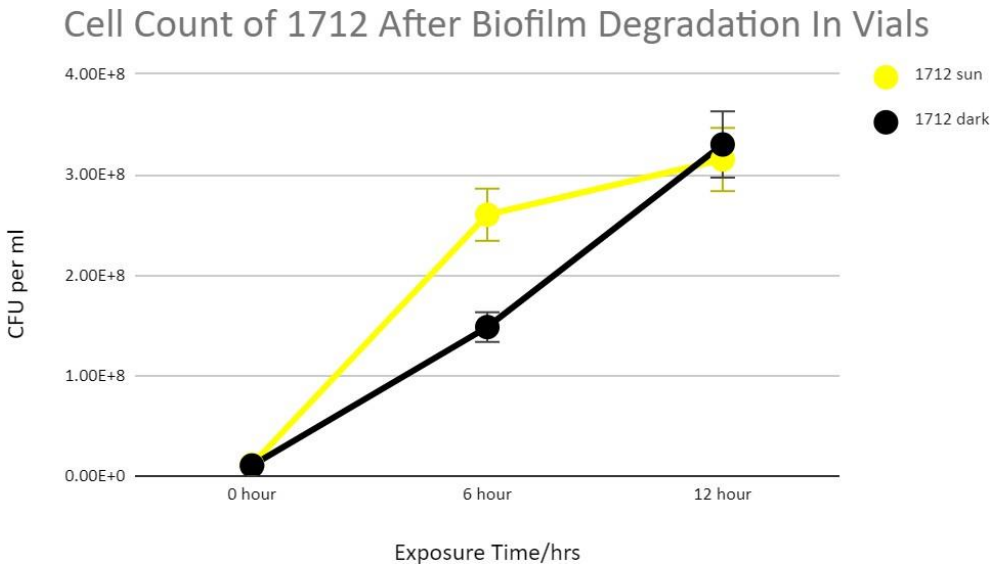

Figure 4.4: Graphical representation of cell count of *Vibrio 1712* after biofilm degradation in sunlight and in darkness taken from phase 1 data. X axis represents the exposure time in hours and Y axis represents CFU per ml

Organism	**R value and interpretation**	**R^2 value and interpretation**	**Regression model and interpretation**
1712 SUNLIGHT	0.938 Strong positive correlation	R^2= 0.88 88.0% of the total variation of the cell count can be explained by the regression model.	y=4.33E+07 + 2.53E+07*x On average, when the time of exposure in sunlight is 0 hour, the cell count is 4.33E+07 CFU/ml and when the time of exposure increases by 1 hour, cell count increases by 2.53E+07 CFU/ml.
1712 DARK	0.997 strong positive correlation	R^2= 0.994 99.4% of the total variation of cell count can be explained by the regression model.	y=2.67E+06 + 2.67E+07*x On average, when the time of exposure in dark is 0 hour, the cell count is 2.67E+06 CFU/ml and when the time of exposure increases by 1 hour, cell count increases by 2.67E+07 CFU/ml.

Table 3: R value, R square value, regression model and their respective interpretations for *Vibrio 1712* exposed to winter sunlight and darkness taken from phase 1 data

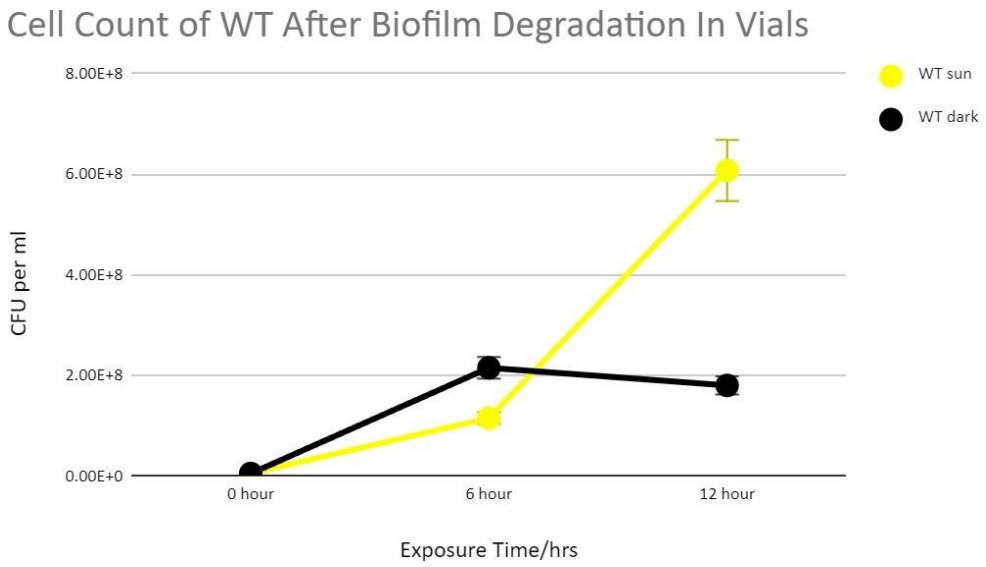

Figure 4.5: Graphical representation of cell count of *Vibrio WT324* after biofilm degradation in sunlight and in darkness taken from phase 1 data. X axis represents the exposure time in hours and Y axis represents CFU per ml

Organism	**R value and interpretation**	**R^2 value and interpretation**	**Regression model and interpretation**
WT 325 SUNLIGHT	0.939 Strong positive correlation	R^2= 0.882 88.2% of the total variation of the cell count can be explained by the regression model.	y=-5.87E+07 + 5.02E+07*x On average, when the time of exposure in sunlight is 0 hour, the cell count is 5.87E+07 CFU/ml and when the time of exposure increases by 1 hour, cell count increases by 5.02E+07 CFU/ml.
WT 325 DARK	0.778 strong positive correlation	R^2= 0.605 60.5% of the total variation of cell count can be explained by the regression model.	y=4.59E+07 + 1.46E+07*x On average, when the time of exposure in dark is 0 hour, the cell count is 4.59E+07 CFU/ml and when the time of exposure increases by 1 hour, cell count increases by 1.46E+07 CFU/ml.

Table 4: R value, R square value, regression model and their respective interpretations for *Vibrio WT324* exposed to winter sunlight and darkness taken from phase 1 data

4.1.3 T-TEST RESULTS FOR BIOFILMS FORMED ON VIALS:

Null Hypothesis: There is no significant difference between cell count in winter sun and winter dark

Alternative Hypothesis: There is a significant difference between cell count in winter sun and winter dark

ORGANISM	Time/Hour	p-value	interpretation	Null hypothesis	Overall remarks
STEC SUN VS STEC DARK	0 6 12	0.138 0.001 0.027	0.138>0.05 0.001<0.05 0.027<0.05	ACCEPT REJECT REJECT	NULL HYPOTHESIS REJECTED
WT 324 SUN VS WT 324 DARK	0 6 12	0.857 0.001 0.001	0.857>0.05 0.001<0.05 0.001<0.05	ACCEPT REJECT REJECT	NULL HYPOTHESIS REJECTED
1877 SUN VS 1877 DARK	0 6 12	0.004 0.001 0.077	0.004<0.05 0.001<0.05 0.077>0.05	REJECT REJECT ACCEPT	NULL HYPOTHESIS REJECTED
1712 SUN VS 1712 DARK	0 6 12	0.618 0.002 0.585	0.618>0.05 0.002<0.05 0.585>0.05	ACCEPT REJECT ACCEPT	NULL HYPOTHESIS REJECTED

Table 5: Statistical significance comparison between the cell counts taken from phase 1 data of biofilms exposed to winter sunlight and winter darkness by T-test

4.1.4 Interpretation of the Statistical Analysis of Phase 1 Data

The graphical representations (Figs. 4.2, 4.3, 4.4) show that the number of cells increases over time in both the dataset exposed to sunlight and the dataset kept in the dark. The only exception is *Vibrio WT*324, where the number of cells decreased in the second six hours for the data set exposed to sunlight (Fig. 4.5). This rise is supported by the r value, which indicates a moderate to strong positive association between cell count and exposure period. The regression models provide quantifiable data for how the cell count increases with each hour of exposure time.

These values are:

8.3E+07 CFU/ml and 3.77E+07 CFU/ml in sunlight and darkness respectively for *STEC*,

2.06E+07 CFU/ml and 8.75E+05 CFU/ml in sunlight and darkness respectively for *Vibrio 1877*,

2.53E+07 CFU/ml and 2.67E+07 CFU/ml in sunlight and darkness respectively for *Vibrio 1712*,

5.02E+07 CFU/ml and 1.46E+07 CFU/ml in sunlight and darkness respectively for *Vibrio WT324* (Table 1-4).

A t-test was performed to determine the amount of significance for the rise in cell count in the data set exposed to sunlight, despite the fact that both the regression model and the graphic representation showed this increase. The t-tests revealed a significant difference in the number of cells between the biofilms kept in darkness throughout the winter and those exposed to sunshine (Table 5). This conclusively shows that the sunlight does significantly break the bacterial biofilms to resuscitate a significant amount of planktonic bacteria during the winter season.This occurs due to the temperature increase then usual temperature in winter season.

4.2.1 PHASE 2: OD of Biofilm Rings Stained with Coomassie Blue

Dye Average OD of stained biofilm exposed to sunlight:

Time/ Bacterial strains	*STEC*	*V. cholerae WT324*	*V. cholerae 1712*	*V. cholerae 1877*
0 hours	0.08725	0.0805	0.08475	0.07475
6 hours	0.07375	0.113	0.07025	0.0765
12 hours	0.0775	0.09225	0.07925	0.08875
18 hours	0.088	0.10825	0.10925	0.11525

Table 6: Average OD of stained biofilm exposed to sunlight, obtained using ELISA at 450 nm

Average OD of stained biofilm exposed to darkness:

Time/ Bacterial strains	*STEC*	*V. cholerae WT324*	*V. cholerae 1712*	*V. cholerae 1877*
0 hours	0.0705	0.167	0.07875	0.0745
6 hours	0.07525	0.08375	0.07075	0.08225
12 hours	0.081	0.0925	0.07825	0.09475
18 hours	0.089	0.118	0.08575	0.09475

Table 7: Average OD of stained biofilm exposed to darkness, obtained using ELISA at 450 nm

4.2.2 Phase 2 Graphs and Regression Analysis

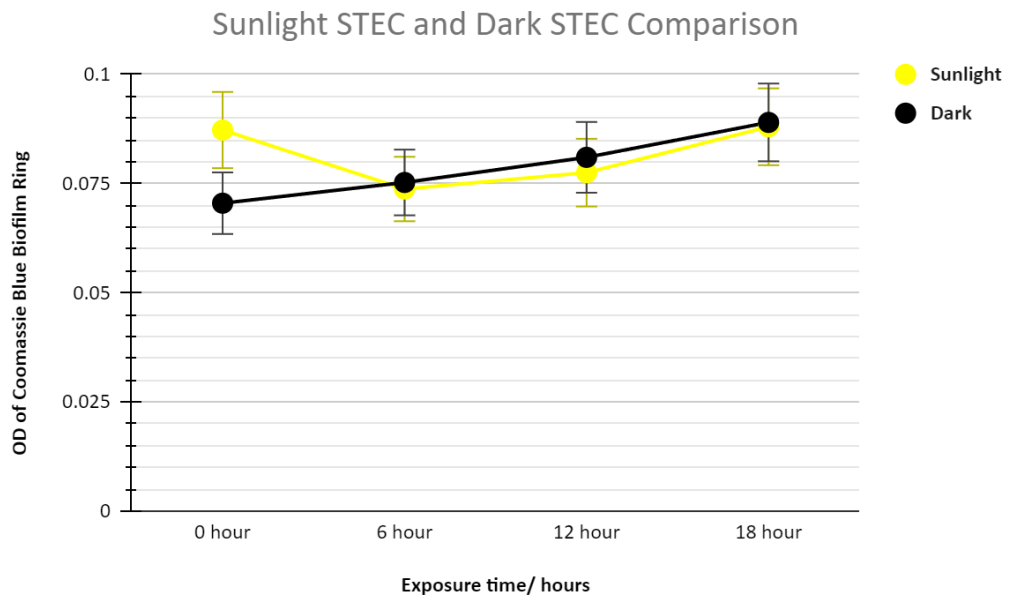

Figure 4.6: Graphical representation of OD of CBB G-250 stained biofilm rings of *STEC* after biofilm degradation in sunlight and in darkness taken from phase 2 data. X axis represents the exposure time in hours and Y axis represents OD of coomassie blue stained biofilm rings

Organism	R value and interpretation	R^2 value and interpretation	Regression model and interpretation
STEC SUNLIGHT	0.109 Weak positive correlation	R^2= 0.012 1.2% of the total variation of OD of biofilm stain OD can be explained by the regression model.	y=0.08+0.0001*x On average, when time of exposure is 0 hour, the OD of biofilm stain is 0.08 and when the time of exposure increases by 1 hour, OD of biofilm stains increases by 0.0001
STEC DARK	0.993 Strong positive correlation	R^2= 0.986 98.6% of the total variation of OD of biofilm stain OD can be explained by the regression model.	y=0.07+0.00102*x On average, when time of exposure is 0 hour, the OD of biofilm stain is 0.07 and when the time of exposure increases by 1 hour, OD of biofilm stains increases by 0.00102

Table 8: R value, R square value, regression model and their respective interpretations for *STEC* exposed to winter sunlight and darkness taken from phase 2 data

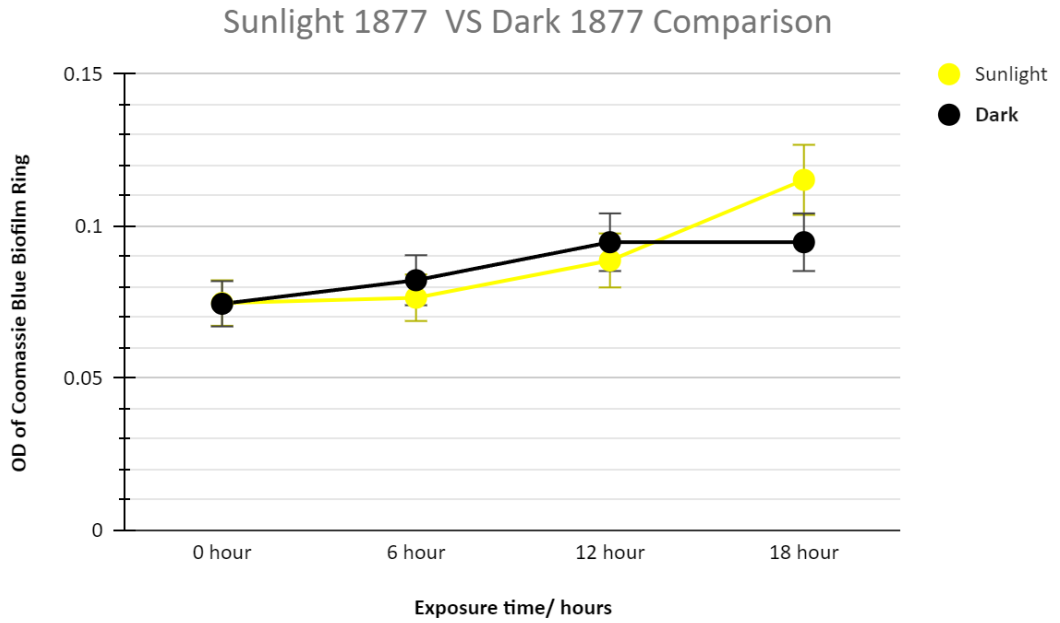

Figure 4.7: Graphical representation of OD of CBB G-250 stained biofilm rings of *Vibrio 1877* after biofilm degradation in sunlight and in darkness taken from phase 2 data. X axis represents the exposure time in hours and Y axis represents OD of coomassie blue stained biofilm rings

Organism	R value and interpretation	R^2 value and interpretation	Regression model and interpretation
1877 SUNLIGHT	0.924 strong positive correlation	R^2= 0.853 85.3% of the total variation of OD of biofilm stain OD can be explained by the regression model.	y=0.07+0.00223*x On average, when time of exposure is 0 hour, the OD of biofilm stain is 0.07 and when the time of exposure increases by 1 hour, OD of biofilm stains increases by 0.00223
1877 DARK	0.949 Strong positive correlation	R^2= 0.9 90% of the total variation of OD of biofilm stain OD can be explained by the regression model.	y=0.076+0.00122*x On average, when time of exposure is 0 hour, the OD of biofilm stain is 0.076 and when the time of exposure increases by 1 hour, OD of biofilm stains increases by 0.00122

Table 9: R value, R square value, regression model and their respective interpretations for *Vibrio 1877* exposed to winter sunlight and darkness taken from phase 2 data

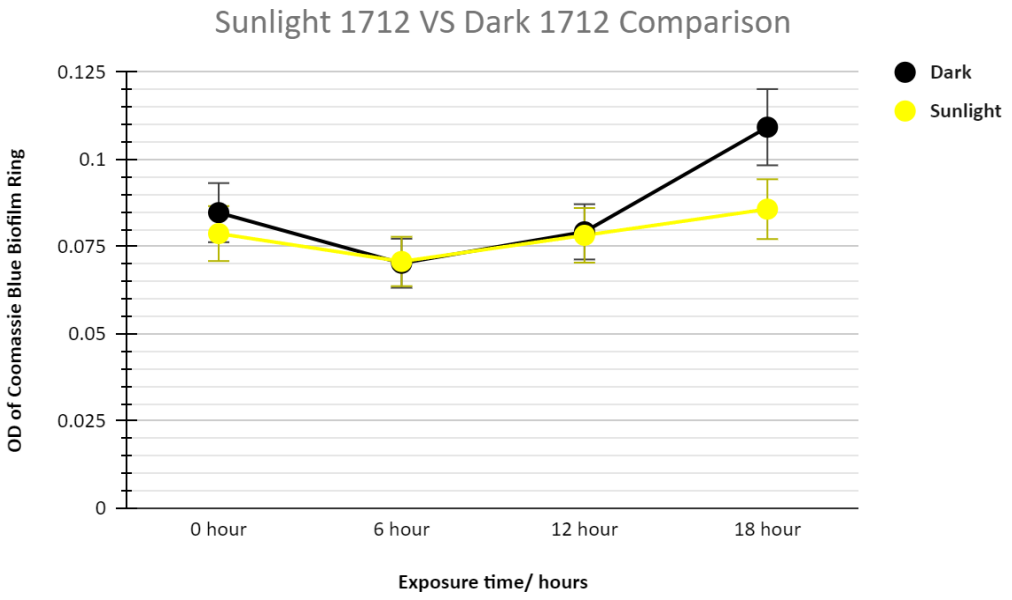

Figure 4.8: Graphical representation of OD of CBB G-250 stained biofilm rings of *Vibrio 1712* after biofilm degradation in sunlight and in darkness taken from phase 2 data. X axis represents the exposure time in hours and Y axis represents OD of coomassie blue stained biofilm rings

Organism	**R value and interpretation**	**R^2 value and interpretation**	**Regression model and interpretation**
1712 SUNLIGHT	0.638 moderate positive correlation	R^2= 0.407 40.7% of the total variation of OD of biofilm stain OD can be explained by the regression model.	y=0.07+0.00137*x On average, when time of exposure is 0 hour, the OD of biofilm stain is 0.07 and when the time of exposure increases by 1 hour, OD of biofilm stains increases by 0.00137
1712 DARK	0.6 moderate positive correlation	R^2= 0.360 36% of the total variation of OD of biofilm stain OD can be explained by the regression model.	y=0.07+0.000475*x On average, when time of exposure is 0 hour, the OD of biofilm stain is 0.07 and when the time of exposure increases by 1 hour, OD of biofilm stains increases by0.000475

Table 10: R value, R square value, regression model and their respective interpretations for *Vibrio 1712* exposed to winter sunlight and darkness taken from phase 2 data

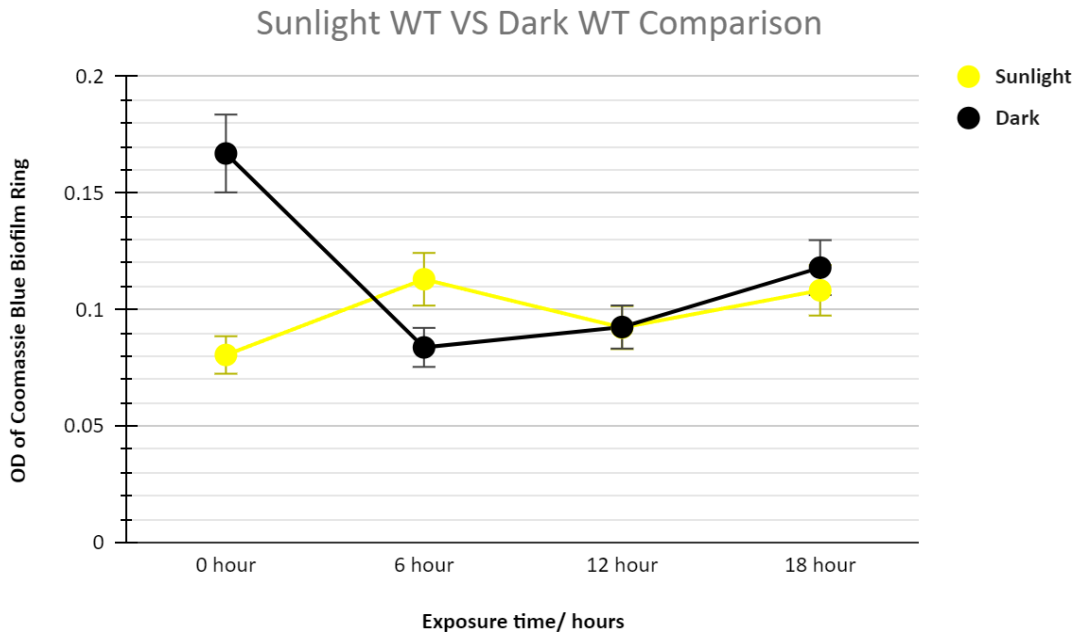

Figure 4.9: Graphical representation of OD of CBB G-250 stained biofilm rings of *Vibrio WT324* after biofilm degradation in sunlight and in darkness taken from phase 2 data. X axis represents the exposure time in hours and Y axis represents OD of coomassie blue stained biofilm rings

Organism	R value and interpretation	R^2 value and interpretation	Regression model and interpretation
WT 324 SUNLIGHT	0.541 moderate positive correlation	R^2= 0.292 29.2% of the total variation of OD of biofilm stain OD can be explained by the regression model.	y=0.09+0.00104*x On average, when time of exposure is 0 hour, the OD of biofilm stain is 0.09 and when the time of exposure increases by 1 hour, OD of biofilm stains increases by 0.00104
WT 324 DARK	-0.477 Weak negative correlation	R^2= 0.228 22.8% of the total variation of OD of biofilm stain OD can be explained by the regression model.	y=0.136-0.0023*x On average, when time of exposure is 0 hour, the OD of biofilm stain is 0.136 and when the time of exposure increases by 1 hour, OD of biofilm stains decreases by 0.0023

Table 11: R value, R square value, regression model and their respective interpretations for *Vibrio WT324* exposed to winter sunlight and darkness taken from phase 2 data

4.2.3 T-TESTS FOR OPTICAL DENSITY OF BIOFILM RINGS STAINED BY COOMASSIE BLUE

Null Hypothesis: There is no significant difference between OD of coomassie rings in winter sun and winter dark

Alternative Hypothesis: There is a significant difference between OD of coomassie rings in winter sun and winter dark

ORGANISM	Time/Hour	p-value	interpretation	Null hypothesis	Overall remarks
STEC SUN	0	0.467	0.47>0.05	ACCEPT	NULL
VS	6	0.638	0.64>0.05	ACCEPT	HYPOTHESIS
STEC	12	0.402	0.40>0.05	ACCEPT	ACCEPTED
DARK	18	0.839	0.83>0.05	ACCEPT	
WT 324	0	0.391	0.39>0.05	ACCEPT	NULL
SUN	6	0.205	0.21>0.05	ACCEPT	HYPOTHESIS
VS	12	0.962	0.96>0.05	ACCEPT	ACCEPTED
WT 324	18	0.658	0.66>0.05	ACCEPT	
DARK					
1877 SUN	0	0.957	0.96>0.05	ACCEPT	NULL
VS	6	0.595	0.60>0.05	ACCEPT	HYPOTHESIS
1877	12	0.554	0.55>0.05	ACCEPT	ACCEPTED
DARK	18	0.475	0.48>0.05	ACCEPT	
1712 SUN	0	0.396	0.40>0.05	ACCEPT	NULL
VS	6	0.937	0.94>0.05	ACCEPT	HYPOTHESIS
1712	12	0.898	0.90>0.05	ACCEPT	ACCEPTED
DARK	18	0.185	0.19>0.05	ACCEPT	

Table 12: Statistical significance comparison between the OD of coomassie blue stained biofilm rings taken from phase 2 data of biofilms exposed to winter sunlight and winter darkness by T-test

4.2.4 Interpretation of the Statistical Analysis of Phase 2 Data

The graphical representations show that both in the dataset that was kept in the dark and in the dataset that was dyed and subsequently dissolved by glacial acetic acid, the optical density of the biofilm rings rises with time under both conditions (Fig.4.6-Fig.4.9). For both the sunlight and dark data sets, the OD increased during each phase of the 18-hour exposure time frame. The increase in OD demonstrates that, after being exposed to light or darkness on a regular basis approximately every six hours, the thickness of biofilm rings has increased. With the exception of STEC biofilm that was kept in the dark, which shows weak negative correlation indicating that the OD does not increase with exposure time, i.e. the biofilm ring does not get thicker, the r value, which shows weak to strong positive correlation between OD and the exposure time, corroborates this increase. The OD increases quantitatively with each hourly increase in exposure time, as seen by the regression models.. These values are:

0.0001and 0.00102 in sunlight and darkness respectively for *STEC*,

0.00223 and 0.00122 in sunlight and darkness respectively for *Vibrio 1877*,

0.00137 and 0.000475 in sunlight and darkness respectively for *Vibrio 1712*,

0.00104 and 0.0023 in sunlight and darkness respectively for *Vibrio WT324 (Table 8-11)*.

As the biofilm rings do not break and the OD of the CBB G250 stain does not decrease, this indicates that exposure to sunlight does not disrupt the bacterial biofilm rings. The t-tests confirm once more how negligible the increases appear to be. A t-test was performed to determine the amount of significance for the increase in OD observed in the data set exposed to sunshine, despite the fact that both the regression model and the graphical representation indicate that this increase occurs. The t-tests show that there is not a significant distinction between the biofilm stains kept in darkness during the winter and those exposed to sunshine in terms of optical density (OD) (Table 12). This conclusively shows that the sunlight does not significantly break the bacterial biofilm rings to decrease its thickness during the winter season.

Chapter 5: Discussion

This research looked into how microorganisms in a biofilm react to sunlight during the winter. Cholera epidemics in Bangladesh are cyclical due to the presence of Vibrio cholerae. Summer is when you're most likely to contract a waterborne illness like cholera, diarrhea, or bloody diarrhea. Biofilms allow these bacteria to persist in the wild all year long. Sunlight in the summer revives the bacterial biofilm, according to previous research. Therefore, the purpose of this research is to determine if exposure to sunshine during the winter can also revive the bacterial biofilm.

5.1 Key findings

It was found that the number of cells in both the sunlight and darkness groups grew with time in both phases 1 and 2. The results suggest an exception, as the cell count for strain *WT324 Vibrio* in phase 1 (vials) decreased after 6 hours of exposure.

The OD of the biofilm rings in phase 2 arose with time when they were dissolved with glacial acetic acid and exposed to sunlight before being kept in the dark. The thickness of the biofilm ring increased during the span of 18 hours. When the *STEC* biofilm was maintained in the dark, the OD did not vary with exposure time, making it the only circumstance in which this was not the case. A statistical analysis of the winter sunlight and dark data sets reveals no significant differences between the data obtained from exposure to sunlight and the data obtained from exposure to darkness. As a result, the collected results support the theory that winter sunlight has minimal impact on the bacterial biofilm.

Statistical analysis of previous research has shown no major difference between the data collected in the previous winter season and the data collected in the current winter season, with the exception of phase 1 data where it was observed that there were significant differences between cell count due to increased temperature compared to previous seasons . The statistical study backs up that there were significant differences between cell counts comparing winter sunlight and darkness. As it was proven that the temperature can change the characteristics of biofilm degradation. Thus, summer sunlight dramatically destroys the bacterial biofilm, leading bacteria to be motile unlike the winter sunlight.

5.2 Interpretations

5.2.1 ***STEC*:** Planktonic bacterial cell count was shown to increase in both the sunlight and darkness exposed datasets during phases 1. There was a considerable rise in cell number between the second and fourth time points depicted in the graphs (Fig:4.2). A high positive connection was found between cell count and exposure time. In addition, the regression analysis indicated that the regression models could account for 89.5% in sunlight and 76.8% of the total variation in the dark data set in phase 1 data, respectively (Table 1). Table 5 demonstrates different rates of growth in cell count and also the t-test reveals statistically significant differences between the data of *STEC* sunlight and dark due to increased temperature. Coomassie stains were used to color the biofilm rings after exposure, and phase 2 data shows an increase in OD for the sunlight-exposed data set and little variation for the darkness-exposed data set. Both sunlight and dark exposure resulted in a steady increase in optical density (OD) of the biofilms (Fig. 4.6), suggesting that the biofilm did not thin out as a result of breakage. Correlation analysis supported the pattern depicted in the graph, showing a weak positive correlation between OD and exposure time for the dataset exposed to sunlight and a strong positive correlation for the dataset exposed to darkness. Regression analysis also indicated that the regression models can account for 98.6% of the total variation in both the bright and dark data sets (Table 8). The t-test revealed no statistically significant differences (Table 12).

5.2.2 ***Vibrio 1877***: According to the result, phase 1 data sets indicate an increase and then a drop in planktonic cell count with time for darkness exposure conditions and linear increase in sunlight. In the first phase, the number of cells increases relatively slowly as a result of being exposed to sunlight (Fig:4.3). Therefore, there appears to be little growth in the overall cell count. For phase 1 the samples exposed to darkness show a sharp elevation in cell count for the first 6 hours of exposure and then a severe decline for phase 1 in the next 6 hours. Additionally, the regression analysis suggested 99.3% of total variation in sunlight data set in phase 1 and 0.0004% of total variation in dark data set from phase 1 respectively can be explained by the regression models (Table 2). Table 5 demonstrates different rates of growth in cell count, but a t-test reveals statistically significant differences between Vibrio 1877 sunlight and dark due to increased temperature. Coomassie stains, which were used to color the biofilm rings after exposure, exhibited an increase in OD in the sunlight-exposed data set but showed negligible change in OD in the dark-exposed data set, per phase 2 results. The biofilms kept in the dark showed a decrease in OD in the last 6 hours of exposure time (Fig:4.7), whereas the

biofilms exposed to sunlight showed a very slow increase in OD, indicating that the biofilm did not get thinner due to breakage. Correlation analysis supported the pattern seen in the visualization, indicating a strong positive correlation between OD and exposure time for the dataset exposed to both sunlight and darkness. Regression analysis also indicated that daylight and darkness accounted for 85.3% and 90% of total variation, respectively. table 9 shows how well each data set is explained by the regression models. The t-test revealed no statistically significant differences (Table 12).

5.2.3 ***Vibrio 1712***: Phase 1 data show a rise in the total number of planktonic bacterial cells, both in the presence of light and in the absence of it. Cell counts were found to be significantly higher in the initial 6 hours of the sunshine data set compared to the later 6 hours (Fig:4.4), whereas the opposite was true for the dark data set. Furthermore, the regression analyses indicated that the regression models could account for 88% for sunlight and 99.4% of the total variation in the dark data set from phase 1 data, respectively (Table 3). In Table 5, a t-test revealed statistically significant differences between Vibrio 1712 sunlight and dark due to increased temperature. After exposure, the biofilm rings were stained with Coomassie blue, however phase 2 data reveal an increase in optical density. Compared to the dark-exposed data set, which shows a consistent incline in OD with time, the sunlight-exposed group's graphical depiction shows a steady increase. 6 hours, peak at 12 hours, and then gradually incline during the following 18 hours (Fig.4.8). Thus, the data reveals the biofilm rings increased thicker with exposure time in both data sets. Correlation analysis supported the pattern depicted in the visualization, indicating a moderately positive correlation between OD and exposure time for both sunlight and dark dataset. Furthermore, Table 10 shows that regression analysis revealed that regression models can account for 40.7% of total variation in the sunlight data set and 36% of total variation in the dark data set. The results of the t-test (Table 12) reveal no significant differences between the sunlight and dark data.

5.2.4 ***Vibrio WT324*****:** The number of planktonic bacterial cells and the amount of time they were exposed to sunlight increased and decreased for darkness between phases 1. During Stage 1, the cell count for both sunlight and darkness increased significantly in the first 6 hours compared to the last 6 hours duration of the dataset for dark where it decreased. There was a consistent increase in the first six hours for the data set that was exposed to dark, and then a steady decrease in the following six hours (Fig. 4.5). Sunlight data showed an almost stable cell count for the first six hours, followed by a dramatic increase for the final six hours (Fig. 4.5). Based on the results of a correlation study,

association between cell count and exposure time was strongly positive in phase 1. Additionally, the regression analyses suggested 88.2% of total variation in sunlight data set in phase 1 and 60.5% of total variation in dark data set from phase 1 can be explained by the regression models (Table 4). In table 5, a t-test revealed statistically significant differences between the dataset of Vibrio WT324 sunlight and dark due to increased temperature. However, in phase 2 data, the OD of Coomassie stains used to stain the biofilm rings after exposure has moderately increased. The graph depicting the dark-exposed data set shows a constant downfall for the first 6 hours, followed by a consistent increasefor the next 12 hours. in sunlight, with the exception of a modest increase in the first 6 hours (Fig. 4.9). Then decreased in the second 6 hours and finally again increased in the last 6 hours. Since the final OD is lower than the initial OD, this implies that the biofilm ring thickness decreased with exposure time in data sets of dark. The correlation analysis, which revealed a modest positive association between OD and exposure time for data sets of sunlight and weak negative for darkness. Regression analysis also indicated that the regression models could account for 22.8of the total variation in the dark data set and 29.2% of the total variation in the sunlight data set (Table 11). The results of the t-test (Table 12) corroborated the findings of the graphical comparison that there are no significant differences between two datasets.

5.3 Limitations:

This study investigated the effects of wintertime sunlight and dark on bacterial biofilm using just four strains of bacteria. A larger number of bacterial strains, especially *Vibrio cholerae* might have made the study's conclusions more broadly applicable. Additionally grown in LB medium were the bacterial strains employed in this research. Determining how sunlight affects the biofilm might be difficult until similar outcomes are obtained with different media.

Furthermore, throughout the period of 3 to 5 weeks, data were gathered for the whole experiment. At every phase of the experiment, more raw information needed to have been collected. Even while this study looking at how winter sunlight affects bacterial biofilm is fascinating, it's vital to remember that other factors could possibly be at work. Even while the identical conditions were kept for both sunlight and dark, the study does not completely rule out the possibility that other factors may have an influence.

Bangladesh experiences two unique cholera outbreaks every year. December and March were the months of both the previous summer study and the present winter research. This implies that the

investigation will not take place for some time. A more complete situation could be achieved with the addition of those months' data.

5.4 Future Prospect of the Research

This study followed up on an earlier one that collected data in summer and winter by collecting data in the current winter. This means that we have a year and half worth of data. In order to draw any firm conclusions, the experiment must now be continued for at least half an year

5.5 Future research

The impact of sunlight on biofilm is the focus of this study. This opens up opportunities for future study to determine which wavelengths of sunlight have the greatest impact on destroying biofilm. More research can be done to determine what sets off the biofilm resuscitation in the summer and why the same mechanism is not as potent in the winter. The impact of winter sunshine on *Vibrio cholerae* biofilm is the primary focus of this investigation. Additional research on the impact of sunlight on biofilm generated by other seasonal diseases is also possible.

Chapter 6: Conclusion

6.0 Conclusion

To conclude, the purpose of this study was to look into how winter sunlight affects bacterial biofilm generated by bacteria responsible for seasonal epidemics. Cholera and diarrhea are seasonal diseases, with peak incidence in the summer and lowest in the winter. These cyclical outbreaks may be linked to the summertime revival of biofilm due to increased solar radiation. Our findings did not support the hypothesis that exposure to sunshine in the winter would significantly disrupt bacterial biofilm. A striking contrast emerged when the same research was repeated in the summer. Thus, the findings suggest that while summer sunlight can revive bacterial biofilm, sunlight during the winter months does not appreciably dissolve bacterial biofilm. Because sunlight does not penetrate the biofilm and release the infectious planktonic bacteria into the environment, cholera and diarrhea are less common in the winter. To confirm this assumption, however, we need more seasonal data.

Chapter 7: References

7.0 References

1. Stepanović, S., Vuković, D., Dakić, I., Savić, B., & Švabić-Vlahović, M. (2000). A modified microtiter-plate test for quantification of staphylococcal biofilm formation. Journal Of Microbiological Methods, 40(2), 175-179.
2. Sultana, M., Nusrin, S., Hasan, N., Sadique, A., Ahmed, K., & Islam, A. et al. (2018). Biofilms Comprise a Component of the Annual Cycle of Vibrio cholerae in the Bay of Bengal Estuary. Mbio, 9(2).
3. Van Houdt, R., & Michiels, C. W. (2005). Role of bacterial cell surface structures in Escherichia coli biofilm formation. Research in microbiology, 156(5-6), 626-633.
4. Vogeleer, P., Tremblay, Y. D., Mafu, A. A., Jacques, M., & Harel, J. (2014). Life on the outside: role of biofilms in environmental persistence of Shiga-toxin producing Escherichia coli. Frontiers in microbiology, 5, 317.
5. Dhaka Wasa must answer for cholera outbreak. The Daily Star. (2022). Retrieved 12 May 2022, from https://www.thedailystar.net/views/editorial/news/dhaka-wasa-must-answer-cholera-outbreak-2993291.
6. Dong, C., Beis, K., Nesper, J., Brunkan, A. L., Clarke, B. R., Whitfield, C., & Naismith, J.H. (2006). The structure of Wza, the translocon for group 1 capsular polysaccharides in Escherichia coli, identifies a new class of outer membrane protein. Nature, 444(7116), 226.
7. E. coli. Who.int. (2018). Retrieved 3 June 2022, from https://www.who.int/news-room/fact-sheets/detail/e-coli.
8. Faruque, S., Naser, I., Islam, M., Faruque, A., Ghosh, A., & Nair, G. et al. (2005). Seasonal epidemics of cholera inversely correlate with the prevalence of environmental cholera phages. Proceedings Of The National Academy Of Sciences, 102(5), 1702- 1707.
9. Alam, M., Sultana, M., Nair, G., Siddique, A., Hasan, N., & Sack, R. et al. (2007). Viable but nonculturable Vibrio cholerae O1 in biofilms in the aquatic environment and their role in cholera transmission. Proceedings Of The National Academy Of Sciences, 104(45), 17801-17806.
10. Baker-Austin, C., Oliver, J. D., Alam, M., Ali, A., Waldor, M. K., Qadri, F., & Martinez- Urtaza, J. (2018). Vibrio spp. infections. Nature Reviews Disease Primers, 4(1), 1- 19.
11. Berk, V., Fong, J. C., Dempsey, G. T., Develioglu, O. N., Zhuang, X., Liphardt, J., & Chu,S. (2012). Molecular architecture and assembly principles of Vibrio cholerae biofilms. Science, 337(6091), 236-239.

12. Bridges, A. A., & Bassler, B. L. (2019). The intragenus and interspecies quorum-sensing autoinducers exert distinct control over Vibrio cholerae biofilm formation and dispersal. PLoS biology, 17(11), e3000429.

13. Del Pozo, J. (2017). Biofilm-related disease. Expert Review Of Anti-Infective Therapy, 16(1), 51-65.

14. Hollmann, B., Perkins, M., & Walsh, D. (2014). Biofilms and their role in pathogenesis. British Society for Immunology. Available online: https://www.immunology.org/public-information/bitesized-immunology/pathogens-andd%20sease/biofilms-and-their-role-in (accessed on 7 August 2020).

15. Huq, A., Whitehouse, C. A., Grim, C. J., Alam, M., & Colwell, R. R. (2008). Biofilms in water, its role and impact in human disease transmission. Current Opinion in Biotechnology, 19(3), 244-247.

16. Karpman, D. (2012). Management of Shiga toxin-associated Escherichia coli-induced haemolytic uraemic syndrome: randomized clinical trials are needed. Nephrology Dialysis Transplantation, 27(10), 3669-3674.

17. Rodger, A., & Sanders, K. (2017). UV-visible absorption spectroscopy, biomacromolecular applications. In Encyclopedia of spectroscopy and spectrometry (pp. 495-502). Elsevier.

18. Silva, A. J., & Benitez, J. A. (2016). Vibrio cholerae biofilms and cholera pathogenesis. PLoS neglected tropical diseases, 10(2), e0004330.

19. Steinberg, T. H. (2009). Protein gel staining methods: an introduction and overview. Methods in enzymology, 463, 541-563.

20. Fong, J. C., Syed, K. A., Klose, K. E., & Yildiz, F. H. (2010). Role of Vibrio polysaccharide (vps) genes in VPS production, biofilm formation and Vibrio cholerae pathogenesis. Microbiology, 156(Pt 9), 2757.

21. Fong, J. N., & Yildiz, F. H. (2015). Biofilm matrix proteins. Microbiology spectrum, 3(2), 3-2.

22. Hall-Stoodley, L., & Stoodley, P. (2005). Biofilm formation and dispersal and the transmission of human pathogens. Trends in microbiology, 13(1), 7-10.

23. Hammer, B. K., & Bassler, B. L. (2003). Quorum sensing controls biofilm formation in Vibrio cholerae. Molecular microbiology, 50(1), 101-104.

24. Lequin, R. M. (2005). Enzyme immunoassay (EIA)/enzyme-linked immunosorbent assay (ELISA). Clinical chemistry, 51(12), 2415-2418.

25. Li, J., Attila, C., Wang, L., Wood, T. K., Valdes, J. J., & Bentley, W. E. (2007). Quorum sensing in Escherichia coli is signaled by AI-2/LsrR: effects on small RNA and biofilm architecture. Journal

of bacteriology, 189(16), 6011-6020.

26. LSR - Lipolysis-stimulated lipoprotein receptor - Homo sapiens (Human) - LSR gene & protein. Uniprot.org. (2006). Retrieved 3 June 2022, from https://www.uniprot.org/uniprot/Q86X29.

27. Mosharraf, F. B., Chowdhury, S. S., Ahmed, A., & Hossain, M. M. (2020). A Comparative Study of Static Biofilm Formation and Antibiotic Resistant Pattern betwe

28. Environmental and Clinical Isolate of Pseudomonas aeruginosa. Advances in Microbiology, 10(12), 663-672.

29. Naser, I. B., Hoque, M. M., Abdullah, A., Bari, S. N., Ghosh, A. N., & Faruque, S. M. (2017). Environmental bacteriophages active on biofilms and planktonic forms of toxigenic Vibrio cholerae: Potential relevance in cholera epidemiology. PLoS One, 12(7), e0180838.

30. Nastasijevic, I., Schmidt, J. W., Boskovic, M., Glisic, M., Kalchayanand, N., Shackelford, S. D., & Bosilevac, J. M. (2020). Seasonal prevalence of Shiga toxin-producing Escherichia coli on pork carcasses for three steps of the harvest process at two commercial processing plants in the United States. Applied and environmental microbiology, 87(1), e01711-20.

31. Pena, R. T., Blasco, L., Ambroa, A., González-Pedrajo, B., Fernández-García, L., López, M., & Tomás, M. (2019). Relationship between quorum sensing and secretion systems. Frontiers in Microbiology, 10, 1100.

32. Preda, V. G., & Săndulescu, O. (2019). Communication is the key: biofilms, quorum sensing, formation and prevention. Discoveries, 7(3).